ECMWF COPERNICUS REPORT

Copernicus Atmosphere Monitoring Service

User Guide to the CAMS Radiation Service (CRS)

Status December 2020

Issued by: DLR / M. Schroedter-Homscheidt

Date: 10/03/2021

Ref: CAMS72_2018SC2_D72.4.3.1_2020_UserGuide_v1.2

Copernicus
Europe's eyes on Earth

IMPLEMENTED BY ECMWF

User Guide to the CAMS Radiation Service

Status December 2020

DLR
Marion Schroedter-Homscheidt
Faiza Azam
Jethro Betcke
Carsten Hoyer-Klick

ARMINES
Mireille Lefèvre
Lucien Wald

TRANSVALOR
Etienne Wey
Laurent Saboret

Please note - the scientific citations for the CAMS Radiation Service are not this User Guide, but the following publications:

- Lefèvre, M. et al, 2013. McClear: a new model estimating downwelling solar radiation at ground level in clear-sky conditions. AMT, 6, 2403-2418, doi: 10.5194/amt-6-2403-2013.
- Gschwind, B., et al., 2019. Improving the McClear model estimating the downwelling solar radiation at ground level in cloud free conditions – McClear-V3., Meteorol. Z., doi:10.1127/metz/2019/0946.
- Qu, Z. et al., 2017. Fast radiative transfer parameterisation for assessing the surface solar irradiance: The Heliosat-4 method, Meteorol. Z., 26, 33-57, doi: 10.1127/metz/2016/0781.

Table of Contents

Executive Summary

The European Earth observation programme Copernicus aims at providing environmental information to support policymakers, public authorities and both public and commercial users. A systematic monitoring and forecasting of the state of the Earth's subsystems is provided within six thematic areas: marine, land, atmosphere, emergency, security, and climate change.

The pre-operational atmosphere service of Copernicus was provided through the FP7 projects MACC and MACC-II/-III (Monitoring Atmospheric Composition and Climate). This is now continued in the operational Copernicus Atmosphere Monitoring Service (CAMS). CAMS combines state-of-the-art atmospheric modelling with Earth observation data to provide information services covering European Air Quality, Global Atmospheric Composition, Climate, and UV and Solar Energy. Within the CAMS Radiation Service (CRS) existing historical and daily updated databases for monitoring incoming surface solar irradiance are made available. The CAMS Radiation Service is subject to a continuous validation and development. The service meets the needs of European and national policy development and the requirements of (commercial) downstream services (e.g. planning, monitoring, efficiency improvements, integration into energy supply grids).

The User Guide describes the data, methods and operations used to deliver time-series of solar radiation available at ground surface.

Section 2 includes a short description of the CAMS Radiation Service ‘in a nutshell’. It is meant for the ‘fast-track readers’ as a first orientation about the available products.

Section 3 describes shortly the previously provided databases HelioClim-3 and SOLEMI. These databases were operated by DLR for SOLEMI and ARMINES and its subsidiary Transvalor for HelioClim-3. The historical evolution of methods used to convert satellite images into solar surface irradiance is shortly presented.

Section 4 describes the Heliosat-4 method, including the McClear model describing the irradiance under clear-sky (cloud-free) conditions, and its different versions. Heliosat-4 is the method used to produce the irradiances in the CRS.

Section 5 intends to summarize existing knowledge and lessons learnt on satellite-based irradiances, which has been published previously only in a scattered manner and was hardly available to users.

Section 6 provides an overview of the operations and the workflow. The products are defined. It also discusses the means to control the quality of the products and the processing chain.

Section 7 defines the method applied in the quarterly validation reports. It discusses the way validation results are presented and how they may be interpreted.

It is intended to update this User Guide regularly.

1. Introduction

The CAMS Radiation Service is designed to meet the requirements that have been expressed for the Copernicus Atmospheric Monitoring Service (CAMS). The precursor projects MACC and MACC-II/-III prepared the CAMS Radiation Service in terms of implementation, sustained operation and availability. They have maintained and further developed the efficiency and resilience of the end-to-end pre-operational system, and have refined the scientific basis and quality of the products of the system. It was ensured that the service lines best meet both the requirements of downstream service providers and end users at the European, national and local levels, and the requirements of the global scientific user community.

The group of CAMS service lines covers air quality, climate forcing, stratospheric ozone, and solar radiation. CAMS delivers operational products and information that support the establishment and implementation of European policy and wider international programmes. CAMS acquires and assimilates observational data to provide sustained real-time and retrospective global monitoring of greenhouse gases, aerosols and reactive gases such as troposphere ozone and nitrogen dioxide. Daily global forecasts of atmospheric composition, detailed air-quality forecasts and assessments for Europe, and key information on long range transport of atmospheric pollutants are provided. Comprehensive web-based graphical products and gridded or time series data is created on which downstream services may be based. Feedback is being given to space agencies and providers of in-situ data on the quality of their data and on future observational requirements.

One of the CAMS services provides radiation values at the ground level, which fulfil the needs in European and national policy developments and the requirements of partly commercial downstream services, e.g., for planning, monitoring, efficiency improvements, and the integration of solar energy systems into energy supply grids.

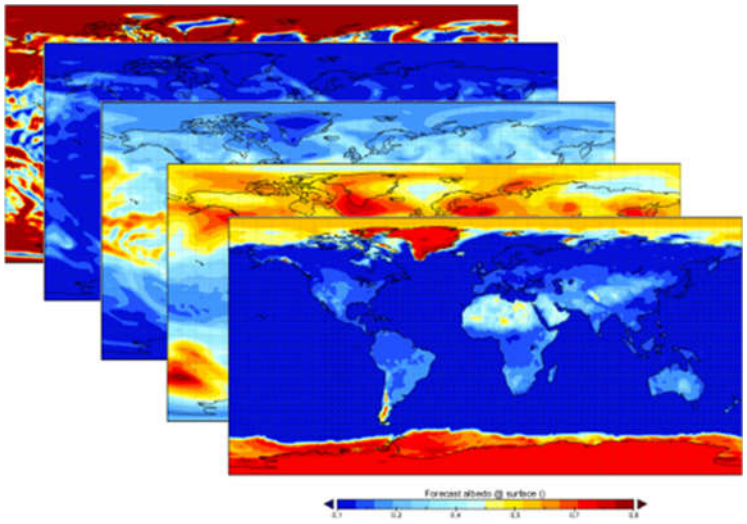

Fig. 1-1: Cascade of various input data layers.

To do so, several data originating from various sources (Fig. 1-1) are assembled. Many of them describe the optical state of the atmosphere, e.g., aerosol optical properties, water vapour and ozone contents over the atmospheric column. Others depict the ground properties, e.g., ground albedo and ground elevation. These data are inputs to a model that simulates the scattering and absorption phenomena occurring in the atmosphere and affecting the solar radiation in its way downwards to the ground. The outputs of this model are values of the solar radiation available at ground level that can be used to produce energy, either as heat or electricity.

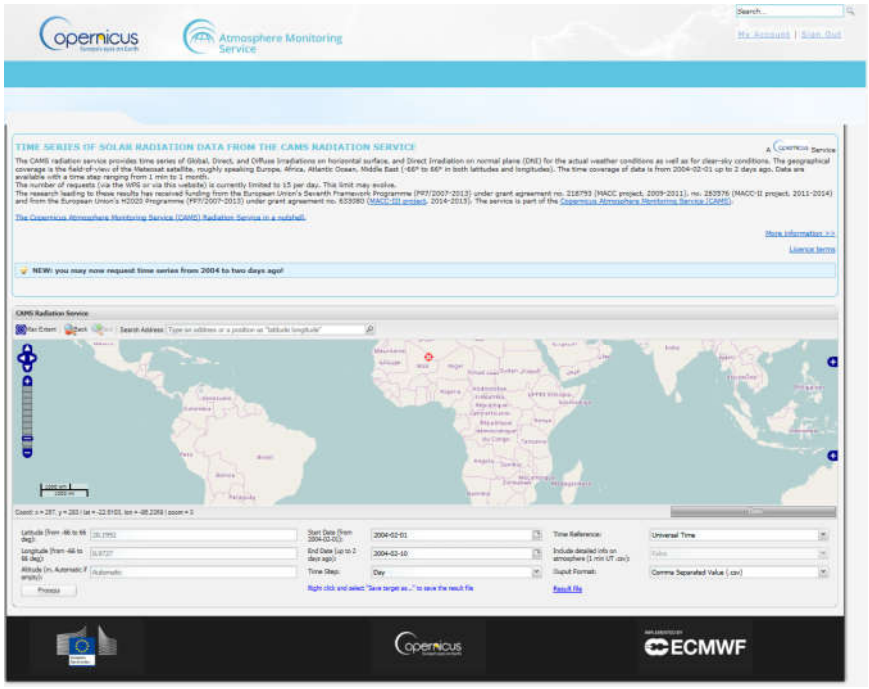

Figure 1-2. Interface of the CAMS Radiation Service

The CAMS Radiation Service (Fig 1-2) products are routinely produced and available through the Atmosphere Data Store. Expected product timeliness, availability, and accuracy are documented and as much in line with user requirements as possible and documented in the Service Specification document. Monitoring of input data, timeliness and availability of output data, and quality of output data against independent observations is in place, where possible. Validation of products is available through Validation reports. The production of the product is monitored 24/7 with analyst support during working hours.

1.1 Objectives of the document

For the sake of simplicity, we denote by CAMS Radiation Service the service within the Copernicus Atmospheric Service that delivers products on solar energy radiation resources.

The objectives of this document are to document the CAMS Radiation Service as well as the user-access procedures to the products delivered by the service.

Actually, such a service is an information system composed of two major blocks. One is made of databases, processing chains, daily operations, methods, input data, controlling and monitoring of operations and quality of products. The other deals with the dissemination of the products, the means of access, control of dissemination and quality of service.

This report documents both blocks. As a service aims at satisfying needs of its users, the specifications of this service must be built on the description of the users expectations on products and delivery, and therefore of their profiles. This is performed within the User Requirement Analysis Document (URAD) as maintained by the CAMS service entity ECMWF (European Centre for Middle-Range Forecasting).

This document intends to be a living one. It will evolve as the service and its components themselves evolve in the CAMS Radiation Service - based on user feedback and own development.

1.2 Acronyms and definitions

ADS	Atmosphere Data Store
CAMS	Copernicus Atmospheric Monitoring Service
CRS	CAMS Radiation Service, a service being operational since 1st January 2016. A service delivering time-series of solar irradiation available at ground level, created by DLR, Armines, and Transvalor within the Copernicus Service. Time-series start on 2004-01-01 and end at current day-2.
DirHI	Direct Irradiance, or Irradiation. Part of the radiation that is received from the direction of the sun on a horizontal plane.
DifHI	Diffuse Irradiance, or Irradiation. Part of the radiation that is received on a horizontal plane from all directions except that of the sun.
DLR	Deutsches Zentrum für Luft- und Raumfahrt e.V., German Aerospace Center
DNI	Direct Normal Irradiance, or Irradiation. Part of the radiation that is received from the direction of the sun by a plane facing the sun.

GHI	Global Horizontal Irradiance, or Irradiation. The radiation that is received by a horizontal plane from all directions.
HelioClim-1	A service and a database containing daily solar irradiation available at ground level, created by Armines from Meteosat images in reduced spatial and temporal resolution. It covers the period 1985-2005.
HelioClim-3	A service and a database containing 15 min solar irradiation available at ground level, created by Armines from Meteosat images. It starts in February 2004 and is updated daily.
Heliosat	Name of a family of methods to convert images acquired by meteorological geostationary satellites into images of solar radiation available at ground level. For example, the databases HelioClim-1 and -3 are constructed with the method Heliosat-2.
Heliosat-4	The new method for computing solar radiation at ground level.
MACC / MACC-II / MACC-III	Monitoring Atmosphere Composition and Climate. Three EC-funded research projects to establish the Copernicus Atmospheric Service.
MACC-RAD Service	The service within the MACC precursor projects that delivered MACC-RAD and McClear products on solar radiation at ground level until the end of 2015.
MACC-RAD	A service delivering time-series of solar irradiation available at ground level, created by Armines and DLR within the MACC / MACC-II / MACC-III projects. Time-series start on 2004-01-01 and end at current day-2. Service delivery was replaced and continued by the CAMS Radiation Service on 1st January 2016.
McClear	A service delivering time-series of solar irradiation that should be observed at ground level if the sky were clear, created by Armines within the MACC / /MACC-II / MACC-III projects. Time-series start on 2004-01-01 and end at current day-2. It is operated now within the CAMS Radiation Service as the cloud-free 'clear-sky' model.
NASA-SRTM	National Aeronautics and Space Administration, Shuttle Radar Topography Mission
SoDa Service	A Web portal offering a one-stop access to several services (databases, applications) relating to solar radiation.
SOLEMI	Solar Energy Mining. It corresponds to both method and service providing SSI.
SSI	Surface Solar Irradiance, also called surface downward solar irradiance, or surface downward shortwave irradiance. It can also denotes irradiation, which is the irradiance multiplied by a duration. For example, hourly irradiation is equal to the hourly average of irradiance multiplied by 3600 s.

2. The CAMS Radiation Service in a nutshell

The atmosphere service of Copernicus combines state-of-the-art atmospheric modelling on aerosols with Earth observation data to provide information services covering European air quality, global atmospheric composition, climate, and UV and solar energy.
The CAMS Radiation Service provides a fast parameterisation of the radiative transfer in the atmosphere (Fig. 2-1) and couples cloud-free sky parameters as aerosols, water vapour, and ozone with satellite-based cloud information (Fig. 2-2).

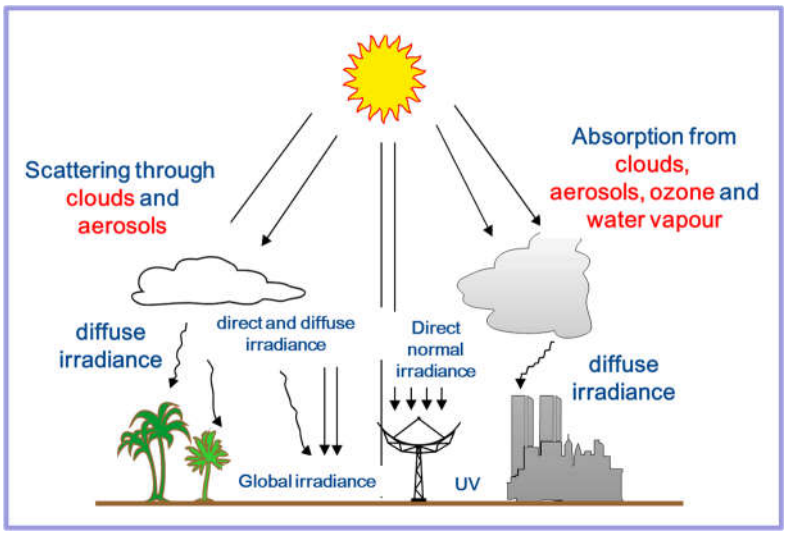

Fig. 2-1: Principle of radiative transfer which is the basis of the CAMS Radiation Service

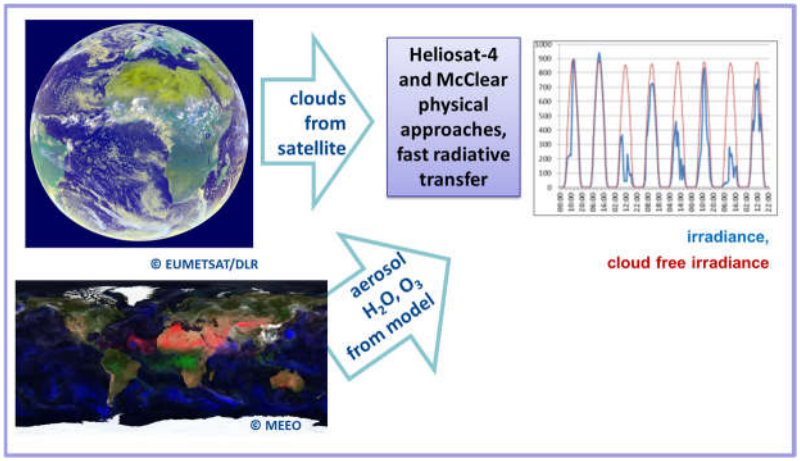

Fig. 2-2: Combination of satellite-based cloud information with model based aerosol, water vapour and ozone information to derive time series of solar radiation at the surface in cloudy and cloud-free conditions

Within the radiation service, existing historical and daily updated databases HelioClim-3 and SOLEMI for monitoring incoming surface solar irradiation were further developed. The CRS is jointly provided by DLR, Armines, and Transvalor. The Monitoring Atmospheric Composition

and Climate (MACC) project series prepared for the service provision, which is now operational as part of the Copernicus programme. Data are made available via the Copernicus Data Store (ADS).

2.1. The CAMS All-Sky Radiation Service in a nutshell

- Period of record: Feb 2004–present, data is provided with up to 2 days delay
- Temporal resolution: 1 min, 15 min, 1 h, day, month
- Spatial coverage: Europe/Africa/Middle East/Eastern part of South America/Atlantic Ocean.
- Spatial resolution: Interpolated to the point of interest
- Data elements and sources: Global, direct, diffuse, and direct at normal incidence irradiation; global, direct, diffuse and direct normal irradiation in cloud free conditions; detailed expert mode with all atmospheric input parameters used for clouds, aerosols, ozone, water vapour, non-bias corrected irradiation values, and the surface reflective properties.
- Data quality control and assessment: Input quality control, regular quarterly benchmarking against ground stations, regular monitoring the consistency and detecting possible trends.
- Availability: Copernicus Atmosphere Data Store https://ads.atmosphere.copernicus.eu.
- Updates: Continuous.
- Data policy: Following the Copernicus data policy – free for any use (see section 4.1)
- Reference: Qu, Z., Oumbe, A., Blanc, P., Espinar, B., Gesell, G., Gschwind, B., Klüser, L., Lefèvre, M., Saboret, L., Schroedter-Homscheidt, M., and Wald L.: Fast radiative transfer parameterisation for assessing the surface solar irradiance: The Heliosat-4 method, *Meteorol. Z.*, 26, 33-57, doi: 10.1127/metz/2016/0781,2017.

2.2. The CAMS Clear Sky Radiation Service in a nutshell

The fast clear-sky model called McClear implements a fully physical modelling replacing empirical relations or simpler models used before. It exploits the recent results on aerosol properties and total column content in water vapour and ozone produced by the Copernicus service. It provides irradiation that would be observed in cloud-free conditions. Data are made available via the Copernicus Atmospheric Data Store (ADS).

- Period of record: 2004–present, data is provided with up to 2 days delay

- Temporal resolution: 1 min, 15 min, 1 h, day, month
- Spatial coverage: Global
- Spatial resolution: Interpolated to the point of interest
- Data elements and sources: clear sky (i.e. cloud free) global, direct, diffuse and direct at normal incidence irradiation; detailed expert mode with all atmospheric input parameters used for clouds, aerosols, ozone, water vapour and the surface reflective properties.
- Data quality control and assessment: Input quality control, regular benchmarking against ground stations, regular monitoring of consistency and detecting possible trends
- Availability: Copernicus Atmosphere Data Store https://ads.atmosphere.copernicus.eu
- Updates: Continuous.
- Data policy: Following the Copernicus data policy – free for any use (see section 4.1).
- References:
  Lefèvre, M., Oumbe, A., Blanc, P., Espinar, B., Gschwind, B., Qu, Z., Wald, L., Schroedter-Homscheidt, M., Hoyer-Klick, C., Arola, A., Benedetti, A., Kaiser, J., W., and Morcrette, J.-J.: McClear: a new model estimating downwelling solar radiation at ground level in clear-sky conditions, *Atmos. Meas. Tech.*, 6, 2403–2418, doi: 10.5194/amt-6-2403-2013, 2013. Available for download at http://www.atmos-meas-tech.net/6/2403/2013/amt-6-2403-2013.pdf
- Gschwind, B., Wald L., Blanc, P., Lefèvre, M., Schroedter-Homscheidt, M., Arola, A., 2019. Improving the McClear model estimating the downwelling solar radiation at ground level in cloud free conditions – McClear-V3., Meteorol. Z./Contrib. Atm. Sci., 28, 2, 147-163, doi:10.1127/metz/2019/0946. Available for download at https://www.schweizerbart.de/papers/metz/detail/28/90593/Improving_the_McClear_model_estimating_the_downwelling_solar_radiation_at_ground_level_in_cloud_free_conditions_McClear_v3

3. The legacy methods

Before proceeding, it is worth mentioning the HelioClim-3 service and the SOLEMI service as two precursor services - called legacy services - which are the foundations of the CAMS Radiation Service. Both, the HelioClim-3 service and the SOLEMI service are fully operational in parallel and managed by Armines and DLR on their own. There is a variety of documentation, validation and user information available for both services – either from standard operations, from recent project related work or from international benchmarking exercises. Therefore, another objective of this user's guide is to combine and summarize this scattered information on satellite-based solar resource data bases. Especially, the lessons learnt on how to or how not to use such a service, are kept in this User Guide in section 5. They are not specific to the CAMS Radiation Service, but they help users in making best usage of the CAMS Radiation Service.

One may see the HelioClim-3 and SOLEMI services as concurrent services. This is true in many aspects. However, Armines and DLR share the same objective: performing research to open-up opportunities for companies. Armines and DLR are not competing on market grounds and have signed a legal agreement in 2008, binding Armines, DLR and Transvalor for the sales of next generation radiation products. This agreement is one of the essential pillars of the consortium providing the CAMS Radiation Service.

3.1. History of the Heliosat methods

Several studies have demonstrated the feasibility of extracting the global solar surface irradiance (SSI) from geostationary satellites images like Meteosat (Tarpley, 1979; Möser and Raschke, 1984). These satellites observe the state of the atmosphere and the cloud cover above the target with passive sensors. These observations can be used to calculate the radiation reaching the ground.

Very early, the European Commission funded research to develop methods for retrieving the SSI from Meteosat images (Grüter et al., 1986). Among those, the Heliosat method was developed at MINES ParisTech (Cano et al., 1986). It became very popular and has been adopted by many researchers. Therefore, it underwent many changes aiming at improvements; the versions bearing major improvements were numbered. The legacy methods are numbered Heliosat-1, Heliosat-2, and Heliosat-3. The CAMS Radiation Service nowadays uses Heliosat-4. Having noticed frequent confusion about the differences among the versions, this chapter aims at an overview on the different precursor versions ('legacy methods'). To our knowledge there is no other single document describing the scientific evolution of the Heliosat algorithm family in a concise manner.

The principles of the legacy Heliosat methods are illustrated in Figure 3.1. In most cases, a cloud exhibits a larger reflectance than the ground. Consequently, the appearance of a cloud in the field of view of the satellite sensor should result in an increase of the perceived signal: the cloud (target 2) appear brighter (whiter) than the ground (target 1). The magnitude of

the difference between both targets is related to the depletion of the downwards radiation by the atmosphere. Of course, the situation where one can compares a cloudy pixel to a neighbour cloud-free pixel rarely happens. Therefore, Heliosat comprises a modelling of the SSI that should be observed by the sensor if the sky were clear for any pixel.

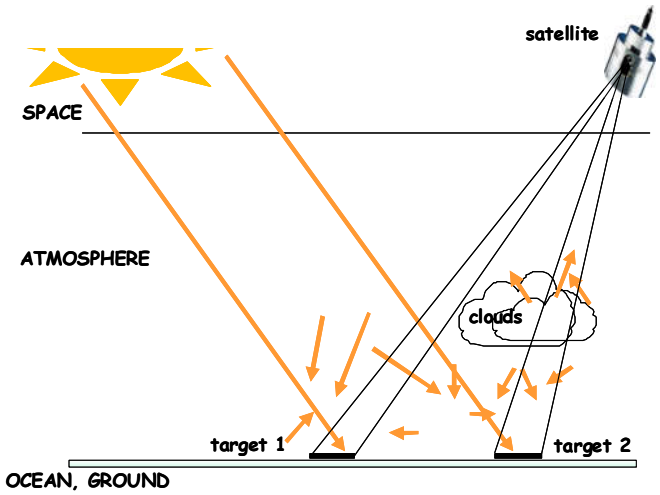

Figure 3.1. Measurement principle as used in cloud-index methods

The legacy versions of Heliosat-1/-2/-3 have in common to be divided into two parts regarding the physical modelling: converting the satellite image into a cloud index and converting the cloud index in irradiance. Therefore, they are called cloud index methods.

The original Heliosat method makes use of the clearness index K_T. K_T is defined as the ratio of the SSI to the irradiance received at the top of the atmosphere. It characterizes the depletion of the solar radiation by the atmosphere. The cloud index n is converted into the clearness index by an empirical affine function $K_T = a\ n + b$, whose parameters a, and b, should be derived empirically by comparison with coincident ground measurements. These parameters can be computed for each location of ground station and then spatially interpolated to produce maps of parameters (Cano et al. 1986). They can also be averaged; the mean values are considered valid for a given region, e.g., Europe (Diabaté et al., 1988). Diabaté et al. (1989) observed that for Europe, three sets of parameters were needed: one for morning, one at noon, and one in the afternoon. A delicate part in the legacy Heliosat method is the determination of the cloud-free instants. As Heliosat-1/-2/-3 use only one channel in visible range, the cloud-free instants should be detected by exploiting the time-series. A cloud-free instant should correspond to a minimum in the time-series, provided all other conditions are equivalent, which is not the case; for example, the sun position is changing within the day and also from day to day for the same hour. Espinar et al. (2009) or Lefèvre et al. (2007) found that a relative error in the ground albedo leads to a relative error of the same magnitude in SSI under clear-sky, i.e., a relative error of order 10 % of the SSI in cloudy cases. Another delicate part in cloud-index based methods is the determination of the albedo of the brightest clouds. The error due to an error in this albedo increases as the

sky is becoming cloudy; consequently, the relative error in the SSI can be very large, e.g., 60 % (Espinar et al., 2009; Lefèvre et al., 2007).

Beyer et al. (1996) at the University of Oldenburg (Germany) produced a version called later Heliosat-1. It enhanced the original Heliosat method in several aspects. The major one is the adoption of the clear-sky index *Kc* instead of the clearness index K_T. The clear-sky index is defined as the ratio of the actual SSI to the SSI that would be received if the sky were clear. The great advantage of the substitution is that the relationship between *Kc* and *n* is universal and is now: *Kc = 1-n*. It has been found by these authors and confirmed by others that little was lost in quality by adopting this relationship for any part of the world and any time. Further work was done to remove partly the dependence of the received radiance with the viewing angle, thus leading to a more spatially-homogeneous cloud-index. In addition, work was performed on the determination of the ground and cloud albedo. Several empirical parameters used in this determination, e.g., the allowed change in time of the ground albedo or the threshold to detect cloud-free instants were revisited and new values were proposed to better account for actual measurements of SSI made by European ground stations.

To improve the accuracy and the reliability of the estimation and to facilitate the implementation of the method, Rigollier et al. (2004) designed the Heliosat-2 version at MINES ParisTech. It exploits the advances proposed by Heliosat-1 and seeks at removing empirical parameters. This is done by adopting several models that have been published independently of Heliosat or Meteosat. This requests a calibration of the Meteosat images to convert gray values into radiances and then reflectances. The clear-sky model proposed in the European Solar Radiation Atlas (ESRA) was adopted (Rigollier et al., 2000). This Heliosat-2 version is presented hereafter.

The Heliosat-3 version has been designed in a collaborative EU-funded project led by University of Oldenburg, and comprising MINES ParisTech and DLR among others. It is characterized by a clear-sky model, called SOLIS, which is an approximation of radiative transfer equations for fast implementation (Mueller et al. 2004).

3.2. Overview of the Heliosat-2 method

Both the legacy databases HelioClim-3 and SOLEMI were constructed by the same Heliosat-2 method, but they differ in the implementation. The concept of the Heliosat-2 method is as follows. The irradiance *I* for an instant *t* and location (*x, y*) is equal to

$$I(t, x, y) = I_c(t, x, y)\, K_c(t, x, y) \qquad (3.1)$$

where $I_c(t, x, y)$ is the irradiance for the clear-sky case; $K_c(t, x, y)$ is called the clear-sky index, is positive, and quantifies the depletion of I_c due to clouds. Thus, the method is based on *1)* a model of irradiance for clear-sky whose results are more or less depleted as a function of the cloud properties to yield actual irradiance. This concept is the basis of many published models outside Heliosat-2 (Rigollier et al., 2004).

The clear-sky index $K_c(t, x, y)$ is computed from the analysis of the Meteosat image at instant t and from the time-series of images prior to the current one. A cloud-index $n(t, x, y)$ is defined:

$$n(t, x, y) = [\rho(t, x, y) - \rho_g(t, x, y)] / [\rho_{cloud}(t, x, y) - \rho_g(t, x, y)] \quad (3.2)$$

where ρ, ρ_{cloud}, and ρ_g are the reflectances respectively observed by satellite for the pixel under concern, the brightest clouds, and the ground. The cloud index is close to 0 when the observed reflectance is close to the ground reflectance, i.e., when the sky is clear. It can be negative if the sky is very clean, in which case ρ is smaller than ρ_g. The cloud index increases as the clouds are appearing. It can be greater than 1 for clouds that are optically very thick.

An empirical relationship was derived from coincident ground measurements and Heliosat-2 results that links n to K_c (Figure 3.2):

$$\begin{array}{ll} n < -0.2 & K_c = 1.2 \\ -0.2 < n < 0.8 & K_c = 1 - n \\ 0.8 < n < 1.1 & K_c = 2.0667 - 3.6667\, n + 1.6667\, n^2 \\ n > 1.1 & K_c = 0.05 \end{array} \quad (3.3)$$

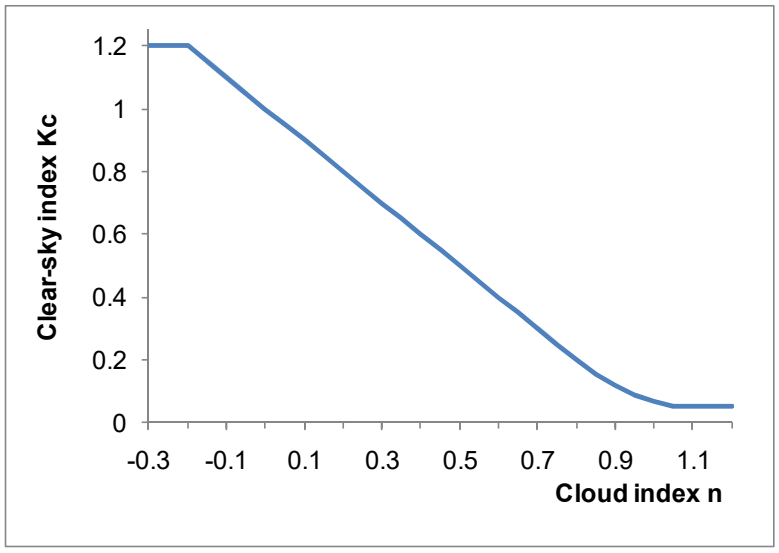

Figure 3.2. Relationship between the cloud index n and the clear-sky index Kc

For the computation of the DNI (direct normal irradiance) in the SOLEMI database, the following equation is used:

$$DNI = DNI_{clear} * exp(a\, n) \quad (3.4)$$

where a is a number which depends on the viewing geometry, the brightness temperatures in thermal infra-red of the pixel, and the spatial variability in the cloud index.

The model of irradiance for clear-sky used for HelioClim is that of the European Solar Radiation Atlas (ESRA); the clear-sky model for SOLEMI (Hoyer-Klick et al., 2016) is the model of Bird (Bird and Hulstrom, 1981) as later been modified by Iqbal (1983) as Model C. Their inputs are discussed in further sections.

There are limitations in the implementation of this concept. One major limitation is that $I_c(t, x, y)$ is unknown. Knowledge on aerosols and other influencing atmospheric parameters is too poor to permit to retrieve on an operational basis the irradiance $I_c(t, x, y)$ for any time and any location. Therefore, the best that can be provided is a typical value of $I_c(t, x, y)$ for this instant and location. In order to cope with that uncertainty, the clear-sky index $K_c(t, x, y)$ is allowed to be greater than 1 while it should not in principle.

The current method Heliosat-2 does not account for the sudden appearance of snow; large errors may appear in the presence of snow cover in cloud-free atmosphere. The satellite derived irradiance values indicate a cloudy sky, since the snow covered pixels appear bright as clouds in the visible channels of the satellite images, as illustrated in Fig 3.3.

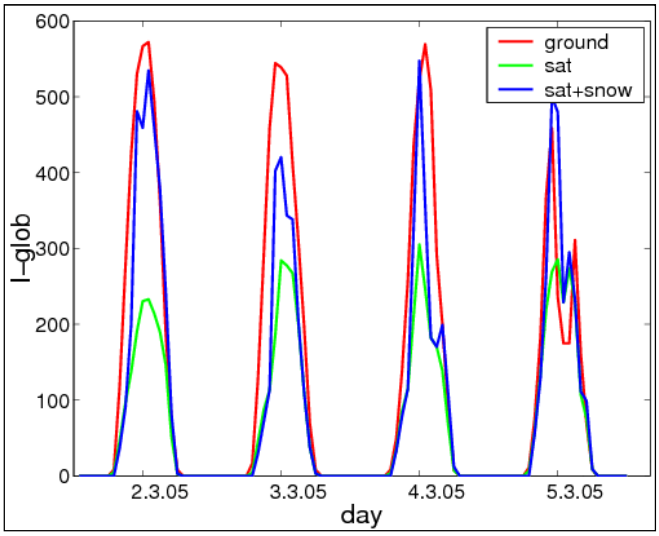

Figure 3.3. Example for satellite derived global irradiance with (blue) and without (green) snow detection in comparison versus ground measured values for a German station in March 2005 (source Univ. Oldenburg).

This figure stands for a German measuring station in March 2005. During this month, the sky was clear for many days and the snow was covering the ground. The ground measurements in red show large values in irradiance, while the SSI retrieved by the Oldenburg method (similar to Heliosat-2) are much too low (in green). An attempt to correct this drawback was successful in this case (blue line).

3.3. Inputs to the clear-sky models

The clear-sky models require external inputs which are discussed in the following sections.

3.3.1. Aerosols

Aerosols have the strongest influence on clear-sky irradiances through absorption and scattering processes. Since aerosol particles are much larger than the solar irradiance wavelength, the scattering processes follow the Mie scattering theory. Unfortunately scattering and absorption processes cannot be well discriminated from each other. Ångstrøm introduced a formula covering both processes that provides the optical thickness as a function of the wavelength λ:

$$k_\lambda = \beta \lambda^{-\alpha} \qquad (3.5)$$

β is the Ångstrøm turbidity coefficient indicating the aerosol content integrated in a vertical column of the atmosphere. The values are usually between 0 and 0.5. α is the wavelength exponent related to the size distribution of the aerosol particles. α usually is between 0.25 and 2.5 with an average of 1.3. Extreme values up to -0.5 or 3.0 are possible.

Modelling aerosols in the atmosphere is very difficult and is one of the major current tasks in atmospheric and climate research. Liu and Pinker (2005) give an overview of the current state of the art. The sources of aerosols are highly variable in space and in time. The interaction of the aerosol particles with the atmospheric trace gases and clouds is complex; the life time is approximately one week and is rather short. Models are making good progress in capturing aerosol evolution, but the characterization of the sources is still difficult (Tanré et al., 2005). Current state-of-the-art data sets currently include satellite observations of aerosols, precursor trace gases, clouds and precipitation and networks of surface-based instruments assimilated into a chemical transport model.

Chemical transport models are off-line models driven by meteorological data or from global circulation models which take aerosol processes as an integral part within the simulation scheme. The available global data sets have made use of satellite data. Many of them have been developed for the use in climate models (Tegen et al. (1997), Kinne et al., 2006, Collins et al., 2001; Zender et al., 2003). Kinne et al. (2001, 2003) give a comparative overview to the different available aerosol data sets.

3.3.2. Water vapour

Water vapour mainly absorbs the solar irradiance in the thermal spectrum and has a larger influence than ozone. The legacy databases used the NCEP/NCAR-Reanalysis of the Climate Diagnostic Center (CDC-NOAA) with a spatial resolution of 2.5° x 2.5°.

3.3.3. Ozone

Ozone absorbs the irradiance predominantly at wavelength lower than 0.3 µm. Therefore the extinction of ozone is fairly low for the complete solar spectrum. The variability of ozone depends mainly on geographical latitude and time of the year. In the solar belt the ozone

concentration is between 0.2 and 0.4 cm[NTP][1],. Since the effect of ozone is very small, a data set from the Total Ozone Mapping Spectrometer (TOMS) sensor was used (McPeters et al., 1998) in the legacy databases.

3.3.4. Linke Turbidity

The Linke turbidity factor (TL, for an air mass equal to 2) is a very convenient approximation to model the atmospheric absorption and scattering of the solar radiation under clear skies. It describes the optical thickness of the atmosphere due to both the absorption by the water vapour and the absorption and scattering by the aerosol particles relative to a dry and clean atmosphere. It summarizes the turbidity of the atmosphere, and hence the extinction of the direct solar radiation (WMO, 1981; Kasten, 1996). The larger TL, the larger the extinction of the radiation by the clear atmosphere.

The Linke turbidity factor denotes the transparency of the cloudless atmosphere. If the sky were dry and clean, TL would be equal to 1. When the sky is deep blue, TL is small. In summer, in Europe, the water vapour is often large and the blue sky is close to white. TL is larger than 3. In turbid atmosphere, e.g. in polluted cities, TL is close to 6 - 7.

A typical value of TL for Europe is 3. However, this value exhibits strong fluctuations in space and time as did the aerosols optical properties and the column-integrated amount of water.

A worldwide database for TL has been proposed by Remund et al. (2003). It has the form of gridded values, whose cells are squared and have a size of 5' of arc angle. There is one grid per month. For a given cell, the value of TL could be considered as representative of the monthly mean value averaged over several years. For a given day, one may interpolate the TL values for the month of this day and the closest month.

One may use the CAMS Clear Sky service to obtain Linke Turbidity Factors from CAMS output. Knowing the clear sky direct irradiance and the extra-terrestrial irradiance, the Lambert-Beer relation can be used to derive an effective optical thickness of a non-dry/non-clear but cloud-free atmosphere this can be used in the definition equation for Linke Turbidity as given e.g. in eq. 9 in Hammer et al. (1998) or in Ineichen and Perez (2002).

3.3.5. Known problems with input data in the legacy databases HelioClim-3 and SOLEMI

Aerosol loading and water vapour amount are difficult to measure with remote sensing methods over land. The retrieval of aerosols is handicapped by the small aerosol reflectance and the perturbation of the weak signal by clouds and surface reflection. It can also be difficult to distinguish between water vapour and clouds. Thus, aerosols and water vapour

1 The unit cm[NTP] refers to the thickness under normal temperature and pressure.

data are usually taken from numerical model reanalyses and the accuracy and resolution are limited. These data have often been available only on a daily or monthly basis and with a resolution close to 1° or coarser in the legacy databases. Furthermore, there were many different data sets available. It was difficult to select a specific one. It may happen that the data set matching most of the validation sites may not be the best for a specific site. Figure 3.4 shows three different aerosol data sets. It can be seen that the absolute values and distributions are very different even if only the annual average is compared.

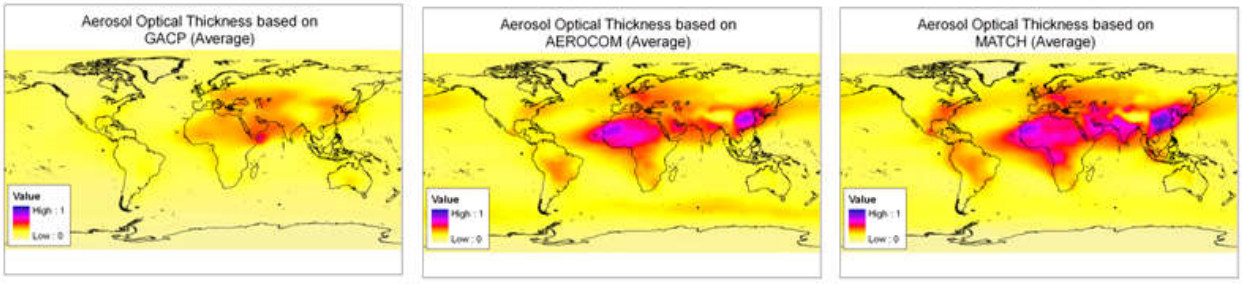

Figure 3.4. Different global annual average aerosol data sets as used in legacy databases. The colour scaling is the same on all three images.

Nonetheless, aerosol loading and water vapour amount are very variable in time and space and have a great influence on SSI, particularly in clear skies. The error induced on the SSI depends on the variation of these parameters within the pixel. The clearer the sky, the greater the error. Comparisons between ground measurements of hourly means of SSI made at sites in Europe less than 50 km apart for clear skies show that the spatial variation in SSI, expressed as the relative root mean square difference, can be greater than 10%.

The main influence on direct irradiance comes from clouds, determined from pictures taken at a distance of 36 000 km. The distinction between different cloud types is very difficult. Observations made by satellite bear a spatial average over pixels; a satellite-derived information of 50% cloud cover for a pixel can result from a 50% semi-transparent homogenous cloud or a broken cloud field with 50% cloud coverage within this pixel. These two cloudy conditions attenuate the radiation in a very different way.

Therefore, models have to make simplifying assumptions to transform the cloud information derived by the satellite into an effective cloud transmission. E.g. the transmission of direct normal irradiance is estimated with a simple exponential function depending on the cloud observations in the visible and infrared channels of the satellite. Figure 3.5 gives such a sample based on the visible cloud index. The applied function may not be the best for all sites and climatic conditions.

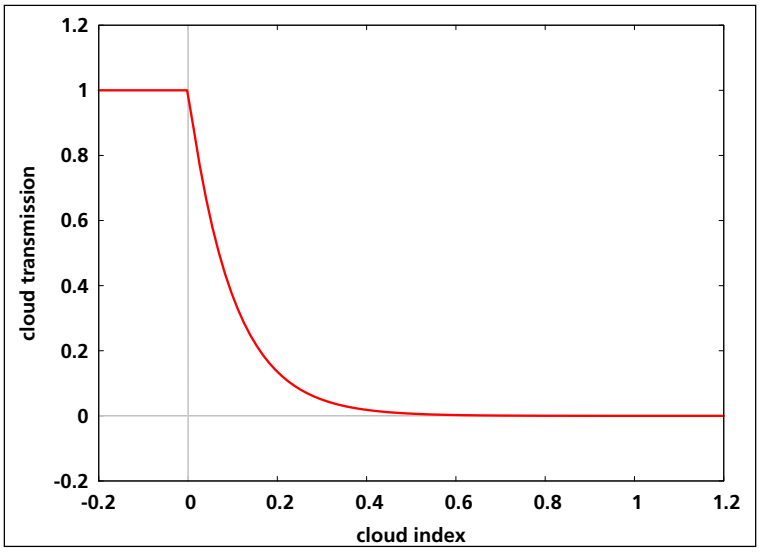

Figure 3.5. Example of transfer function from cloud observation (cloud index) to cloud transmission.

The variability in space and time has been reported in the scientific literature. For example, Wielicki and Welch (1986), Rossow and Schiffer (1999) note typical scale of variation of 30 m and 10 min. This is smaller than the spatial and temporal sampling in the Meteosat images.

This section clearly demonstrates one of the previous limitations of the legacy methods for assessing the irradiance. The inputs used so far for the construction of the legacy databases SOLEMI or HelioClim-3 are climatological values, whether they are aerosol properties and water contents or Linke turbidity factors. These climatologies cannot account for the daily variability or the day-to-day variability of these parameters.

These inputs have a major influence on the value of the clear-sky SSI. The lack of variability impacts the quality of the retrieval of the SSI at daily and smaller time-scales. The impact is enhanced in the case of the DNI (direct irradiance at normal incidence).

The poor availability of accurate inputs is a recurrent problem. The CAMS Service provides these inputs by the means of the ECMWF/CAMS IFS model suite. The integration of CAMS clear sky parameters is a major step forward from the legacy processing chains towards the CAMS Radiation Service.

4. The Heliosat-4 method

Compared to the legacy methods Heliosat-1/-2/-3 and the legacy databases HelioClim-3 and SOLEMI, the CAMS Radiation Service makes now use on a physical retrieval of cloud parameters and a fast parameterization of radiative transfer in the Heliosat-4 method. This is a major change in the version history.

The new Heliosat-4 method (Qu et al., 2016) estimates the down-welling shortwave irradiance received at ground level in all sky conditions. It provides the global irradiance and its direct and diffuse components on a horizontal plane and the direct irradiance for a plane normal to sun rays. It is a fully physical model using a fast, but still accurate approximation of radiative transfer modelling and is therefore well suited for geostationary satellite retrievals. It is composed of two models based on abaci, also called look-up tables: the McClear (Lefèvre et al., 2013; Gschwind et al., 2019) model calculating the irradiance under cloud-free conditions and the McCloud model calculating the extinction of irradiance due to clouds. Both have been realized by using the libRadtran (Mayer and Kylling, 2005) radiative transfer model.

The main inputs to Heliosat-4 are aerosol properties, total column water vapour and ozone content as provided by the CAMS global services every 3 h (Benedetti et al., 2009; Inness et al., 2013; Morcrette et al., 2009; Remy et al., 2019). Cloud properties are derived from images of the Meteosat Second Generation (MSG) satellites in their 15 min temporal resolution using an adapted APOLLO (AVHRR Processing scheme Over cLouds, Land and Ocean, Kriebel et al., 1989; Kriebel et al., 2003) scheme as further described in Qu et al. (2016).

4.1. Concept of Heliosat-4

The Heliosat-4 method is based on the decoupling solution proposed by Oumbe et al. (2014). They have shown that in the case of infinite plane-parallel single- and double-layered cloud, the solar irradiance at ground level computed by a radiative transfer model can be approximated by the product of the irradiance under clear atmosphere and a modification factor due to cloud properties and ground albedo only. Changes in clear-atmosphere properties have negligible effect on the latter so that both terms can be calculated independently.

Let G denote the global SSI for any sky. G is the sum of the beam component B of the SSI – also known as the direct component– and of the diffuse component D, both received on a horizontal surface. Let note G_c, B_c and D_c the same quantities but for clear-sky. The ratios K_c and K_{cb} are called clear-sky indices:

$$K_c = G / G_c \qquad (4.1)$$
$$K_{cb} = B / B_c$$

K_c is also called cloud modification factor in studies on UV or photosynthetically active radiation. The indices K_c and K_{cb} concentrate the cloud influence on the downwelling radiation and are expected to change with clear-atmosphere properties P_c since the clouds and atmospheric constituents are mixed up in the atmosphere. Eq. 9.1 can be expanded:

$$G = G_c(\theta_S, \rho_g, P_c)\, K_c(\theta_S, \rho_g, P_c, P_{cloud}) \qquad (4.2)$$
$$B = B_c(\theta_S, P_c)\, K_{cb}(\theta_S, P_c, P_{cloud})$$

where

- Θ_S is the solar zenithal angle,
- ρ_g the ground albedo,
- P_c is a set of 7 variables governing the optical state of the atmosphere in clear-sky: *i)* total column contents in ozone and *ii)* water vapour, *iii)* elevation of the ground above mean sea level, *iv)* vertical profile of temperature, pressure, density, and volume mixing ratio for gases as a function of altitude, *v)* aerosol optical depth at 550 nm, *vi)* Angström coefficient, and *vii)* aerosol type,
- P_{cloud} is a set of variables governing the optical state of the cloudy atmosphere: *i)* cloud optical depth (τ_c), *ii)* cloud phase, *iii)* cloud liquid water content, *iv)* droplet effective radius, and *v)* the vertical position of the cloud.

Oumbe et al. (2014) have quantified the error made in decoupling the effects of the clear atmosphere from those due to the clouds in cloudy sky, i.e. if changes in P_c are neglected in K_c, respectively K_{cb} in Eq. 9.2. This is equivalent to say that the first derivative $\partial K_c / \partial P_c$, resp. $\partial K_{cb} / \partial P_c$, is close to 0. In that case, Eq. 9.2 may be replaced by the following approximation:

$$G \approx G_c(\theta_S, \rho_g, P_c)\, K_c(\theta_S, \rho_g, P_{c0}, P_{cloud}) \qquad (4.3)$$
$$B \approx B_c(\theta_S, P_c)\, K_{cb}(\theta_S, P_{c0}, P_{cloud})$$

where P_{c0} is an arbitrarily chosen but typical set P_c. The error made in using this approximation depends mostly on the solar zenithal angle, the ground albedo and the cloud optical depth and is less than 2% in relative value for most cases. The maximum error (percentile 95%) on global and direct irradiances is less than 15 W m^{-2}. The errors made are similar to those recommended by the World Meteorological Organization for high quality measurements of the solar irradiance.

These results are important in the view of an operational system as it permits to separate the whole processing into two distinct and independent models, whose inputs are different. Each part of the equation can be processed following the available spatial and temporal resolutions of their inputs. This is of practical importance in CAMS. CAMS clear sky parameters are typically provided only every 3 h. Their spatial resolution is in the range 50 km - 150 km. On the other hand, the cloud properties are derived from the processing of Meteosat images with an adapted APOLLO chain. Such products are available every 15 min for each Meteosat pixel. Therefore, having two different modules for clear-sky and cloudy atmospheres, eases the burden of coping with these differences in resolution and availability.

4.2. Schematic view of the Heliosat-4 method

In Heliosat-4 (Fig. 4.1) two models are used: McClear for the clear-sky (which is defined as being cloud-free) irradiances G_c and B_c, and McCloud for computing the clear-sky indices K_c and K_{cb} in cloudy conditions.

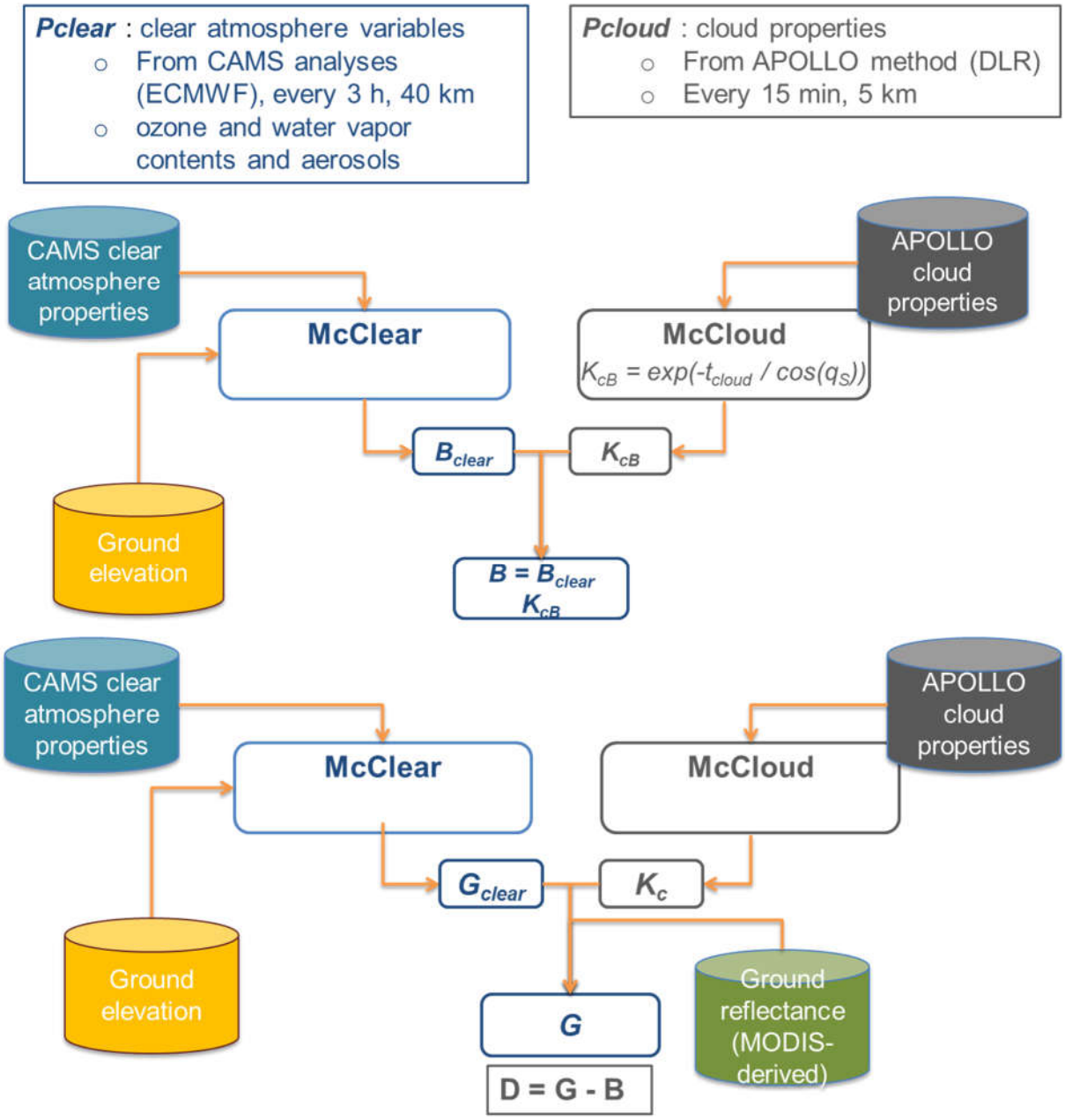

Figure 4.1. Schematic view of the Heliosat-4 method for direct (upper panel), global and diffuse (lower panel) irradiances

4.3. Overview of the McClear model

The fast clear-sky model called McClear (Lefèvre et al., 2013) estimates the downwelling shortwave direct and global irradiances received at ground level under cloud-free skies. Within the Heliosat algorithm family, cloud-free skies are traditionally named 'clear sky' and this terminology is kept even if very turbid conditions in e.g. a dust aerosol event may not appear to be 'clear sky'.

McClear implements a fully physical modelling replacing empirical relations or simpler models used before (e.g. as described in section 3). It exploits the recent results on aerosol properties, and total column content in water vapour and ozone produced by the CAMS global service. It accurately reproduces the irradiance computed by the libRadtran reference radiative transfer model with a computational speed approximately 10^5 times greater by adopting the abaci, or look-up tables, approach combined with interpolation functions. It is therefore suited for geostationary satellite retrievals or numerical weather prediction schemes with many pixels or grid points, respectively.

Based on the input data availability in the CAMS service, McClear delivers time-series of SSI for any place in the world and any instant starting from 2004.

The McClear model and its products are part of the CAMS All-Sky Radiation Service and are used as such. For example, they are used to improve the quality of the HelioClim-3 database adopted by many professionals in solar energy following the method proposed by Qu et al. (2014) thus leading to the HelioClim-3v5 database. Several assessments of the quality of the outputs of McClear v2 have been made (Eissa et al., 2015; Lefèvre, Wald, 2016; Lefèvre et al., 2013; Qu et al., 2014). In addition, HelioClim-3v5 outputs have been exploited in several occasions to provide maps of solar radiation that are hosted by the Global Atlas at the International Renewable Energy Agency (IRENA).

Several drawbacks have been identified during these assessments and daily operations. Hence, a new version v3 was implemented on 2017-10-11 (Gschwind et al., 2019). McClear v3 follows the same concept than McClear v2. It is a fast parameterization of the radiative transfer in the cloud-free atmosphere and it was intended to reproduce the results of the libRadtran code. This parameterization is based on the use of abaci that contain results of libRadtran for specified inputs.

Inputs to McClear v3 are:

- θ_S as provided by the fast algorithm for the solar position SG2 (Blanc and Wald, 2012);
- three parameters describing the bidirectional reflectance distribution function (BRDF) in the Moderate-resolution Imaging Spectroradiometer (MODIS) database (Schaaf et al., 2002) from which ρ_g can be computed. The worldwide climatological monthly means of these three parameters as derived by Blanc et al. (2014) from the MODIS BRDF/Albedo

model parameters product MCD43C1 and MCD43C2 data have been used. This dataset has a spatial resolution of 0.05°;

- the altitude of the ground level, given by the user, or taken from the SRTM data set (Farr et al., 2004) if available or the GTOPO30 data set (Gesch and Larson, 1996);
- the elevation of the CAMS cell above the ground;
- the total AOD at 550 nm and the partial optical depths at 550 nm for dust, organic, sea salt, sulphate, and black carbon aerosol species from CAMS;
- the total column contents in ozone and water vapour given by CAMS;
- the vertical profiles of temperature, pressure, density, and volume mixing ratio for gases as a function of altitude, which are those from the USA Air Force Geophysics Laboratory (AFGL, Anderson et al. 1986) as implemented in libRadtran: tropics, mid-latitude summer and winter, and sub-Arctic summer and winter. A zoning has been constructed for the automatic selection of the atmospheric profile for any site based on the Koeppen climate classification map (Lefèvre et al., 2013). In order to avoid spatial discontinuity due to the abrupt change in vertical profiles, the original algorithm of Lefèvre et al. (2013) has been improved. McClear computes G_c and B_c for each profile and averages these estimates weighted by the inverse of the distance of the site of interest to the closest border of each zone. The period ranging from November to April is considered as boreal winter and austral summer.

Compared to McClear v2, the main change in inputs deals with the aerosol properties. In v2, the partial aerosol optical depths were used to empirically define the aerosol type in the following: urban, continental clean, continental polluted, continental average, maritime clean, maritime polluted, maritime tropical, Antarctic, and desert. Now, the partial aerosol optical depths are directly used in the libRadtran model.

McClear irradiances were compared to 1 min measurements made in clear-sky conditions in several stations within the Baseline Surface Radiation Network in various climates. For global, respectively direct, irradiance, the correlation coefficient ranges between 0.95 and 0.99, resp. 0.86 and 0.99. The bias is comprised between -6 and 25 W m^{-2}, resp. -48 and +33 W m^{-2}. The RMSE ranges between 20 W m^{-2} (3% of the mean observed irradiance) and 36 W m^{-2} (5%), resp. 33 W m^{-2} (5%) and 64 W m^{-2}2 (10%). These results are better than those from the clear-sky model used in the HelioClim-3 legacy service. The study demonstrates the quality of the McClear model combined with CAMS global products, and indirectly the quality of the aerosol properties modelled by the CAMS global reanalysis and forecasts. When both versions v2 and v3 are compared, results are similar with limited changes in performances in global, direct or diffuse irradiances.

Compared to McClear v2, McClear v3 removes several discontinuities:

- those induced by abrupt changes in the aerosol mixtures due to the empirical algorithm;

- those in time due to abrupt changes from winter to summer and reciprocally in the adopted atmospheric profiles;
- those with changing solar zenithal angles induced by the piece-wise MLB functions. In addition, McClear v3 has extended the estimation of the diffuse irradiance to solar zenith angle greater than 90°.

By changing the treatment of the aerosols, McClear v3 is ready to better accommodate possible future changes in the aerosol outputs from the CAMS global forecasting system. McClear v3 removes the ambiguity in McClear v2 induced by the use of the Angstroem exponent in conjunction with the mixtures. Other changes are the adoption of the latest version of libRadtran (V2.0.1) and of a change in the solar constant (now, called total solar irradiance in many papers).

As a whole, compared to v2, McClear v3 offers more consistent results with no more discontinuity. It is a significant step that prepares further improvements, especially from changes in modelling the aerosol optical depth.

4.4. Overview of the McCloud model

The clear-sky index for direct radiation K_{cb} is computed as a function of the cloud optical depth τ_c.

$$K_{cb} = exp[-\tau_c / cos(\theta_S)] \quad (4.4)$$

K_c is computed by the means of a look-up table approach combined with interpolation functions between the nodes of the tables. Another result from MACC and MACC-II projects is that the vertical position of clouds and their geometrical thickness have a very small effect on *G.* As a consequence, typical altitudes of clouds may be selected instead of updated and localized values. Four types of clouds have been selected as this information is provided by the APOLLO scheme, as described later:

- low cloud: water cloud at low altitude. The cloud base height is 1.5 km and the geometrical thickness is 1 km,
- medium cloud: water cloud at medium altitude. The cloud base height is 4 km with a thickness of 2 km,
- high cloud: water cloud of large vertical extent from low altitude to medium altitude. The cloud base height is 2 km and the thickness is 6 km,
- thin ice cloud: ice cloud with a base height of 9 km and a geometrical thickness of 0.5 km.

High clouds, such as *cumulonimbus* which extend vertically from 1 and 2 km up to the tropopause (8-10 km), are mostly composed by water droplets and may have a cloud top

made of ice crystals. They are currently treated as water clouds though it has been found later that more accurate results are attained if these clouds are treated as two-phase clouds.

No information on the droplet effective radius and cloud liquid water content is currently operationally available in the CAMS Radiation Service – this will only be available after the foreseen change towards using the APOLLO_NG (APOLLO Next Generation, Klüser et al., 2015). Currently, typical values of 20 μm and 0.005 g m^{-3} for ice clouds and 10 μm and 1.0 g m^{-3} for water cloud are used.

Four abaci were constructed containing values of K_c, one for each type of cloud. The node points in an abacus are:

- solar zenithal angle Θ_S (deg): 0, 5, 10, 15, 20, 25, 30, 35, 40, 45, 50, 55, 60, 65, 70, 75, 80, 85, 89,
- cloud optical depth τ_c: 0.1, 0.5, 1, 2, 3, 4, 6, 8, 10, 13, 16, 20, 25, 30, 37, 45, 55, 65, 75, 90, 110, 140, 180, 230, 290, 370, 500,
- ground albedo ρ_g: 0, 0.1, 0.9.

The abaci were computed by running libRadtran with 'DISORT 16 stream' as solver. Inputs to libRadtran were the nodes listed above, and a typical set P_{c0} defining the state of the clear atmosphere:

- the middle latitude summer from the USA Air Force Geophysics Laboratory (AFGL) data sets is taken for the vertical profile of temperature, pressure, density, and volume mixing ratio for gases as a function of altitude,
- aerosol properties: optical depth at 550 nm is set to 0.20, Angström coefficient is set to 1.3, and type is continental average,
- total column content in water vapour is set to 35 kg m^{-2},
- total column content in ozone is set to 300 Dobson unit,
- elevation above sea level is 0 m.

Radiative transfer as used here assumes that clouds are infinite and made of plane-parallel layers. In reality three-dimensional cloud effects as e.g. the parallax effect (Schutgens and Roebeling, 2009; Greuell and Roebeling, 2009) and the overshooting of global irradiances (Schade et al., 2007) are observed. These effects are also very sensitive to the geometrical height, the extension and the overall structure of the cloud, but cannot be treated by plane-parallel radiative transfer simulations. Nevertheless, in the operational geostationary satellite-based irradiance retrievals, the necessary input on three-dimensional cloud structures is mostly unavailable. Therefore, these effects are not included here.

In the CAMS Radiation Service, cloud physical properties are provided by APOLLO (AVHRR Processing scheme Over cLouds, Land and Ocean; Kriebel, Saunders, and Gesell, 1989; Kriebel et al., 2003). This algorithm was originally developed to exploit data from the AVHRR

sensors aboard the polar orbiting series of NOAA satellites, in order to estimate the properties of clouds. It has been adapted at DLR to process images of SEVIRI (Spinning Enhanced Visible and Infrared Imager) instrument aboard the series of Meteosat Second Generation satellites (Qu et al., 2016). APOLLO provides quantities related to cloud for each pixel (3 km at nadir) and every 15 min. Among these quantities, there are a mask of cloud-free/cloudy, τ_c and the type of the cloud as low, medium, high, or thin ice. Cloud coverage, i.e. the fraction of a pixel covered by a cloud, expressed in per cent, is derived separately. The retrieval of physical properties is only possible for fully cloudy pixels. Physical properties for partially cloudy pixels are interpolated from neighbouring fully cloudy pixels and weighted with the cloud coverage.

4.5. Computation of the SSI

The two first interpolations on θ_S and τ_c provide three values of K_c, one for each ρ_g = 0, 0.1, and 0.9. McClear provides the corresponding three values of G_c. G is computed for each of the three ρ_g:

$$G(\theta_S, \rho_g, P_{c0}, P_{cloud}) = G_c(\theta_S, \rho_g, P_{c0})\, K_c(\theta_S, \rho_g, P_{c0}, P_{cloud}) \quad (4.5)$$

Let note K_T the clearness index, also called global transmissivity of the atmosphere, or atmospheric transmittance, or atmospheric transmission, defined as:

$$K_T = G / E_0 \quad (4.6)$$

where E_0 denotes the irradiance received on a horizontal surface at the top of atmosphere for the location and time under concern. The formula of Vermote et al. (1997):

$$K_T(\rho_g) = K_T(\rho_g=0)/ (1 - \rho_g\, S_{cloud}) \quad (4.7)$$

describes the change in KT as a function of the ground albedo ρ_g and the spherical albedo S_{cloud} of the cloudy atmosphere. S_{cloud} is unknown and in principle, it can be computed using Eq. 9.7 knowing $KT(\rho_g)$, or equivalently $G(\rho_g)$, for any value of ρ_g. In practice, it is sufficient to know $E(\rho_g)$ for three values of ρ_g: 0.0, 0.1, and 0.9, and S_{cloud} can be computed for any ρ_g by linear interpolation and extrapolation:

$$S_{cloud}(\rho_g=0.1) = [1 - G(\rho_g=0)/ G(\rho_g=0.1)] / 0.1 \quad (4.8)$$
$$S_{cloud}(\rho_g=0.9) = [1 - G(\rho_g=0)/ G(\rho_g=0.9)] / 0.9$$
$$a = [S_{cloud}(\rho_g=0.9) - S_{cloud}(\rho_g=0.1)] / 0.8$$
$$b = S_{cloud}(\rho_g=0.1) - 0.1\, a$$
$$S_{cloud} = a\, \rho_g + b$$

and finally

$$G(\theta_S, \rho_g, P_c, P_{cloud}) = G(\rho_g=0) / [1 - \rho_g\, S_{cloud}]$$
$$= G_c(\theta_S, \rho_g=0, P_c)\, K_c(\theta_S, \rho_g=0, P_{c0}, P_{cloud}) / [1 - \rho_g\, S_{cloud}] \quad (4.9)$$

4.6. Practical implementation

The ground albedo ρ_g is computed in the same way as in Lefèvre et al. (2013). Blanc et al. (2014) created a worldwide climatological complete database containing monthly means of the three BRDF parameters, called *f*iso, *f*vol, and *f*geo (Schaaf et al., 2002). There is one value of each parameter per month which is allotted to the middle of the day of the middle of the month. A linear interpolation yields *f*iso, *f*vol, and *f*geo for each minute of the day.

In the presence of cloud, ρ_g is not the same as that calculated by McClear and must be computed again. The major difficulty is that ρ_g depends upon $D(\rho_g)$ and $G(\rho_g)$ which depend themselves on ρ_g. At this step, B, and accordingly KT_B, are known, and the method proposed by Lefèvre et al. (2013, Eq. 8) can be used to solve the problem.

Solar zenithal angle θ_S and extra-terrestrial irradiance E_0 are computed with the SG2 algorithm (Blanc and Wald, 2012) for the middle of the minute.

Aerosol properties, and total column contents of water vapour and ozone in the CAMS Radiation Service are given every 3 h, starting at 00:00 UT. The ordering of interpolation of parameters was found as having a negligible influence on the results (Lefèvre et al., 2013). A bi-linear spatial interpolation in space is applied to compute a time-series of 3 h values for the given location. A further linear interpolation in time is performed yielding time-series of these atmospheric quantities every 1 min. The 1 min temporal resolution has been chosen as it reflects the variability of irradiation due to the solar position sufficiently well.

Cloud type and τ_{cloud} from APOLLO/SEV are given every 15 min for each pixel of the MSG image. The abacus for the cloud reference category is applied. A series of abacus-internal interpolations is performed to yield K_{cB} and K_{cG} for three ρ_g (=0, 0.1, 0.9) for the 1 min that contains the exact instant of the view of the specific pixel.

Finally, all irradiance parameters are computed every 1 min. If needed, they are summed up to the requested temporal output resolution and irradiation of 15 min, 1 h, 1 day, or 1 month.

4.7. Bias correction

Several publications have dealt with the validation of the CAMS Radiation Service. Qu et al. (2016) focused on 15 min global, direct and diffuse irradiations acquired at BSRN sites. Thomas et al. (2016a) performed a similar validation with BSRN sites but for 1 h summarization time and other years. Thomas et al. (2016b) and Marchand et al. (2016) deal with 1 h global irradiation for specific regions, respectively, Brazil, and Oman and UAE. These authors reported that the correlation coefficients between the ground measurements and the estimates are large, in full agreement with the numerous quarterly validation reports in the CAMS. It is proven that the CAMS Radiation Service offers accurate estimates of of the SSI provided every 15 min. The correlation coefficients for CAMS Radiation Service are very similar to those reached by the commercial services HelioClim-3v4 and v5. It may be

concluded that CAMS Radiation Service has reached a high degree of maturity regarding the ability to reproduce the SSI at various summarizations, from 15 min up to 1 day and more.

The articles mentioned above report that the relative bias of global irradiance is often positive and large, noting an overestimation by the CAMS Radiation Service. On the contrary, the retrieval of the direct irradiance usually exhibits an underestimation. A bias correction was developed and implemented on 2017-10-11 (version 3).

The update consists in performing an on-the-fly post-processing of the original values delivered by the CAMS Radiation Service in order to correct them before the delivery to the user. The post-processing consists in two abaci, one for the global irradiance and one for the direct irradiance. Given an original time-series of outputs from the CAMS Radiation Service, one computes the corresponding time-series of clearness index, direct clearness index and solar zenithal angle. These three quantities are the entries of the abaci, which in turn provide two quantities that are added to respectively the clearness index and direct clearness index. These indices are converted into corrected irradiances. These corrected irradiances are added into the original times-series. The corrected time-series are eventually delivered to the user.

The main argument for a bias correction is that CAMS Radiation Service time series are easier to use without any additional effort. The drawback is that any statistical post-processing cannot be removed by expert users anymore, which would like to apply their own statistical post-processing e.g. when additional ground observations are available at the location of interest. Currently, there is a full transparency about all input and output parameters as they are all provided in the ‘detailed info’ expert output mode. This is a value in itself and should be kept. Therefore, both the non-bias corrected and the bias corrected irradiances are provided in the ‘detailed info’ expert output mode. The standard output mode provides only the bias-corrected irradiances.

5. Known problems in the retrieval of the SSI

Radiative transfer in the atmosphere is a complex phenomenon. In an operational method for the assessment of the SSI, methods should run fast at the expenses of the complexity of the models and therefore of the accuracy of the retrieved SSI. For example, several interactions between radiation and ground (e.g. reflections on the surrounding slopes) or clouds (reflections on the sides of clouds, multi-layered clouds, etc.) are currently not taken into account.

5.1. Sub-pixel phenomena

There will be an error when the actual conditions differ from the average state. The frequency (15 min) of satellite observations is very satisfactory to describe the transitional phenomena such as convection even if only a snapshot is taken. But the size of the pixel is not adapted to the micro-meteorology. There is a spatial integration which smooths the phenomena. Meteosat pixels have actually an elliptic shape and their average diameter ranges from 3 km to 7 km depending on the viewing geometry of the satellite. The resolution at the sub satellite point is 3 km at ground. Figure 5.1 shows a typical Meteosat Second Generation pixel with N-S extent of about 5 km and E-W extent of about 4 km in Central Europe. In this example, one can note the presence of clouds in the ellipse, whose size is much lower than the pixel size.

Figure 5.1. Typical satellite pixel in Europe with sizes of about 4x5 km².

Rapid changes in cloud cover can be noticed in ground measurements, especially at 1 min sampling steps. The spatial heterogeneity resulting from a patchwork of scattered clouds (e.g. cumulus) may induce a characterisation as cloud free by APOLLO/SEV because of the spatial integration effect.

5.2. Change in terrain elevation within a grid cell in databases

The computation of the SSI from satellite images calls upon a digital terrain model (DTM) whose cell size fits that of the pixel. Actually, the CAMS Radiation Service asks the user for the altitude of the site. If the information is not provided, then three different DTMs are

exploited. This is permitted because the computation is performed on-the-fly. If the site of interest is covered by the DTM SRTM with a spatial resolution of approximately 100 m, then SRTM is used. If not, the DTM GTOPO30 with a resolution of 0.5' of arc angle is used. If not, the DTM TerrainBase (TerrainBase 1995) whose cell size is 5' of arc angle, i.e. approximately 10 km at mid-latitude, is exploited.

In very steep relief, irradiance additionally depends upon cast shadows on the site by surrounding obstacles (Figure 5.2) and not only on the change in altitude.

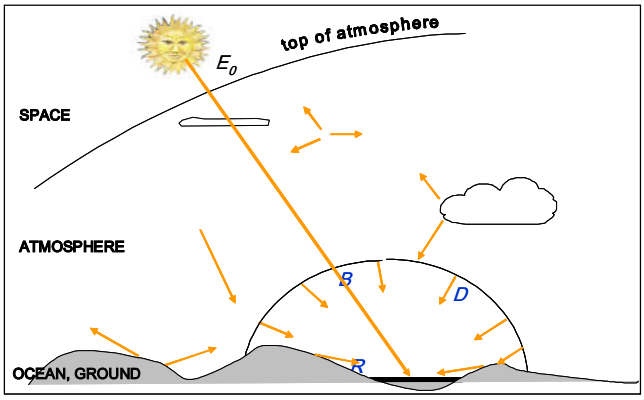

Figure 5.2. Incident irradiance in a complex terrain. B: direct irradiance; D: diffuse irradiance; R: irradiance reflected by nearby terrain

Figure 5.2 shows that the SSI on a horizontal surface is composed of the direct irradiance, diffuse irradiance partly masked by the surrounding mountains, and a reflected part R due to the reflexion on the surrounding slopes. Most often, if not always in operational methods, R is not accounted for; the irradiance calculations are done under the assumption of a flat terrain within the pixel. This applies also for the CAMS Radiation Service. In that case, the tilt angle α and azimuth angle β of the element receiving the radiation are set to 0 and the cosine of the local incident angle θ is:

$$\cos\theta(0,0) = \cos\omega \cos\delta \cos\phi + \sin\delta \sin\phi \qquad (5.1)$$

where ω is the hour angle, δ is the solar declination, and ϕ is the latitude of the site.
In case of non-flat pixel, for each element (*dx, dy*) within a pixel, the cosine of the local incident angle θ is:

$$\cos\theta(\alpha, \beta) = (\cos\omega \cos\delta \cos\phi + \sin\delta \sin\phi) \cos\beta + \cos\omega \cos\delta \sin\phi \cos\alpha \sin\beta + \sin\omega \cos\delta \sin\alpha \sin\beta - \sin\delta \cos\phi \cos\alpha \sin\beta \qquad (5.2)$$

where α and β correspond to the direction of the local slope, respectively in azimuth and tilt. Thus, the SSI of the pixel should be modified by the ratio *R'*:

$$R' = \iint_{pixel} \cos\theta(\alpha(x, y)),\beta(x, y)) \, dx \, dy \, / \cos\theta(0,0) \qquad (5.3)$$

5.3. Coastal sites

Similar to the effect as described in section 5.1 and 5.2, any coastal site may be affected by the inhomogeneity inside the satellite pixel. Such cases are mixed pixels with parts of land and parts of ocean surface and may be misclassified as a cloud. Different thresholds are applied over open sea water than over land as open sea water is typically darker than land surfaces and also than shallow water close to the coast. In the next software version, a filter will be implemented that treats shallow water like land surfaces to better avoid coastal clouds.

5.4. Satellite viewing angles larger than 60°

Retrieval quality degradation with respect to cloud properties is caused by large satellite viewing angles. Locations close to the maximum field of view of MSG are typically on the very edge of the valid domain of the cloud retrieval scheme APOLLO/SEV. The plane-parallel approximation of radiative transfer is not valid anymore and errors due to the parallax effect become important (Schutgens and Roebeling, 2009; Laguarda et al., 2020). The parallax effect shifts the clouds actually covering the site northwards (in the northern hemisphere) and the sensor aboard the satellite does not see the actual atmospheric conditions along the exact optical path between the sun and the station of interest. Additionally, the cloud is seen from the side which contrasts with the plane-parallel assumption made. The quality of cloud physical properties is especially reduced when the sun is low above horizon, e.g. in wintertime, or in early morning and late afternoon. Also, the automatic surface snow/cloud differentiation is more likely to fail. Nevertheless, it has been decided to provide the data in those regions even if large biases are expected as several users have applications where the drawbacks are acceptable. The stations Florianopolis (Brazil) and Toravere (Estonia) are used in the regular quarterly validation reports to quantify this effect.

5.5. Bidirectional reflectance and albedo

Reflexion properties of the ground are a function of the incident and viewing angles. Up to now, these parameters are not operationally available in a high temporal resolution. The CAMS Radiation Service e.g. makes use of monthly maps.

Figure 5.3 shows the angular variation of the reflectance of a coniferous forest in the near infrared (Oumbe 2009). The change in reflectance with the angles can be large; it is greater than 0.1 in Figure 5.3. It can be much larger in the specific case of oceans, where the reflectance depends also on wind speed and varies from values close to zero to values greater than cloud reflectance (Lefèvre et al., 2007). By considering the hemispherical albedo instead of the bidirectional reflectance, one commits a significant error on the part of irradiance reflected by the ground then backscattered by the atmosphere, thus contributing to the diffuse fraction of the SSI. This omission is very often made for operational reasons because of the lack of data describing the ground.

A similar effect can be found in case of clouds because cloud reflectance changes with illuminating and viewing angles due to both the scattering phase function of the cloud and a viewing geometry from the side on the cloud.

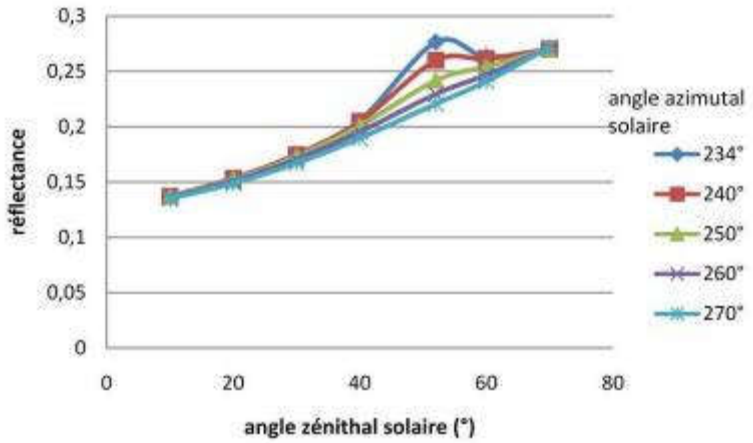

Figure 5.3. Example of variation in ground reflectance with the solar zenithal angle. Viewing and azimuthal angles are set to 52° and 234°, respectively.

5.6. Cloud vertical position

Contrary to objects at ground, clouds are located at different altitudes in the atmosphere. If the viewing angle is large, i.e. far from the satellite nadir, the parallax effect becomes noticeable for not too vertically extended clouds at medium and high altitudes. This results in an erroneous assessment of the geographical position of the cloud. The cloud will be assigned to a pixel farther from the nadir of the sensor than the actual one. The pixel over which the cloud is actually located will be seen as a cloud-free pixel and the SSI assessment will be inaccurate. In the individual case, the vertical position of the cloud top and bottom is not known exactly enough to allow a parallax correction. Mean values could be assumed, but have not proven to be successful in the whole MSG field of view and for the MSG multispectral pixel resolution. Therefore, Heliosat-4 does not perform any parallax correction.

5.7. Cloud detection over bright and cold desert surfaces

In winter conditions clear-sky instants in the early morning or the late afternoon at desert locations are sometimes mistaken as clouds. A desert pixel may be seen as cold in the thermal and bright in the visible channels and therefore, it may be misinterpreted as cloud. Such cases have been observed e.g. for stations in Israel or Morocco.

5.8. Systematic biases if comparing against BSRN ground observations

The Baseline Surface Radiation Network (BSRN, Ohmura et al., 1998) is frequently used as validation database for irradiances. The spectral range of instruments used in the BSRN network is 285 to 2800 nm for pyranometers of Kipp & Zonen and 295 to 2800 nm for those of Eppley. This is slightly different from the spectral range in Heliosat-4 which is 240 to 4606 nm following Kato et al. (1999). According to simulations performed with libRadtran, this difference in spectral range induces a bias of 3-8 W m^{-2} in GHI, i.e. an overestimation by Heliosat-4.

This spectral difference affects Heliosat-4 through the McClear model, given the construction of Heliosat-4. Specific abaci were constructed to create a specific, non public, version of McClear v3 that delivers irradiances for the limited range [285, 2800] nm. This version is used for specific validation usages for scientific publication, control and monitoring of the CRS.

5.9. Circumsolar irradiance

There are several definitions of the direct normal irradiance DNI (Blanc et al., 2014). Ground-based measurements made by pyrheliometers oriented towards the sun typically have an aperture half-angle of approximately 2.5°. These instruments collect parts of the radiation coming from the circumsolar region. On the contrary, DNI estimated by radiative transfer models as is the case of Heliosat-4 is valid for a sun being considered as a point source and defining direct irradiance as consisting of non-scattered photons only. The difference between the two is defined as the circumsolar irradiance fraction within the pyrheliometer aperture half-angle.

In clear-sky conditions, the intensity of this circumsolar irradiance fraction is less than 10 W m^{-2} in most cases (Oumbe et al., 2012) and is fairly similar to the uncertainty of the instruments. In ice cloud or heavy aerosol conditions, the relative contribution of the circumsolar irradiance to B_N measured by pyrheliometers may exceed 50%. This explains a large part of the negative bias of B_N and KT_{BN} as found in Qu et al. (2016), and the general overestimation of diffuse irradiances.

It is desirable to bring a correction to K_{cB} estimated by Heliosat-4 when comparing to ground measurements. Building on the work of Shiobara and Asano (1993) and Reinhardt et al. (2012), Qu (2013) proposed an empirical correction applying to K_{cB} when the cloud coverage of a pixel is greater than or equal to 50% by multiplying τ_{cloud} in Eq. 4 by 0.45 for thin ice clouds and 0.75 for all other cloud types. He found a reduction in bias for B_N and KT_{BN}. Though promising, the study was of limited extension and more work is needed on the applicability of this correction and its integration in Heliosat-4. Currently, both DirHI and DNI will be systematically underestimated, while the DifHI will be overestimated.

6. The CAMS Radiation Service

6.1. Data policy

The following 'Licence to Use the Copernicus Atmosphere Monitoring Service Products' applies:

1. Definitions

1.1. '*Licensor*' means the European Union, represented by the European Centre for Medium-Range Weather Forecasts (ECMWF).

1.2. '*Licensee*' means all natural or legal persons who agree to the terms of this Licence.

1.3. '*Licence*' means this license agreement between the Licensor and the Licensee as amended from time to time.

1.4. '*Copernicus Services*' means:

1.4.1. the Copernicus Atmosphere Monitoring Service (CAMS), which is to provide information on air quality on a local, national, and European scale, and the chemical composition of the atmosphere on a global scale.

1.4.2. the Copernicus Climate Change Service (C3S), which is to provide information to increase the knowledge base to support policies on adaptation to and mitigation of climate change

1.5. '*Copernicus Products*' means all products listed in the C3S or CAMS Service Product Specification or any other items available through an ECMWF Copernicus portal, except those items which are labelled/flagged as being subject to their own separate terms of use.

1.6. '*Intellectual Property Rights*' refers to intellectual property rights of all kinds,

1.6.1. including: all patents; rights to inventions; copyright and related rights; moral rights; trademarks and service marks; trade names and domain names; rights in get-up; rights to goodwill or to sue for passing off or unfair competition; rights in designs; rights in computer software; database rights; rights in confidential information (including know-how and trade secrets); any other rights in the nature of intellectual property rights;

1.6.2. in each case whether registered or unregistered and including all applications (or rights to apply) for, and renewals or extensions of, such rights and all similar or equivalent rights or forms of protection which subsist or will subsist now or in the future in any part of the world together with all rights of action in relation to the infringement of any of the above.

1.7. '*Copernicus Contractor*' refers to providers of Copernicus related goods and services to ECMWF, including information and data, to the Licensor and/or to the users.

1.8. '*Copernicus Regulations*' refers to Regulation (EU) No 377/2014 of the European Parliament and of the Council of 3 April 2014 establishing the Copernicus Programme.

1.9. '*ECMWF Agreement*' refers to the agreement between the European Commission and ECMWF dated 11 November 2014 on the implementation of CAMS and C3S.

2. Introduction

Copernicus is funded under the Copernicus Regulation and operated by ECMWF under the ECMWF Agreement. Access to all Copernicus (previously known as GMES or Global Monitoring for Environment and Security) Information and Data is regulated under Regulation (EU) No 1159/2013 of the European Parliament and of the Council of 12 July 2013 on the European Earth monitoring programme, under the ECMWF Agreement and under the European Commission's Terms and Conditions. Access to all Copernicus information is regulated under Regulation (EU) No 1159/2013 and under the ECMWF Agreement.

3. Terms of the Licence

This Licence sets out the terms for use of Copernicus Products. By agreeing to these terms the Licensee agrees to abide by all of the terms and conditions in this Licence for the use of Copernicus Products.

4. Licence Permission

4.1. This Licence is free of charge, worldwide, non-exclusive, royalty free and perpetual.

4.2. Access to Copernicus Products is given for any purpose in so far as it is lawful, whereas use may include, but is not limited to: reproduction; distribution; communication to the public; adaptation, modification and combination with other data and information; or any combination of the foregoing.

5. Attribution

5.1. All users of Copernicus Products must provide clear and visible attribution to the Copernicus programme. The Licensee will communicate to the public the source of the Copernicus Products by crediting the Copernicus Climate Change and Atmosphere Monitoring Services:

5.1.1. Where the Licensee communicates or distributes Copernicus Products to the public, the Licensee shall inform the recipients of the source by using the following or any similar notice:

'*Generated using Copernicus Climate Change Service information [Year]*' and/or
'Generated using Copernicus Atmosphere Monitoring Service information [Year]'.

5.1.2. Where the Licensee makes or contributes to a publication or distribution containing adapted or modified Copernicus Products, the Licensee shall provide the following or any similar notice:

'Contains modified Copernicus Climate Change Service information [Year]'; and/or
'Contains modified Copernicus Atmosphere Monitoring Service information [Year]'

5.1.3. Any such publication or distribution covered by clauses 5.1.1 and 5.1.2 shall state that neither the European Commission nor ECMWF is responsible for any use that may be made of the Copernicus information or data it contains.

6. Intellectual Property Rights
6.1. All Intellectual Property Rights in the Copernicus Products belong, and will continue to belong, to the European Union.

6.2. All Intellectual Property Rights of new items created as a result of modifying or adapting the Copernicus Products through the applications and workflows accessible on the ECMWF Copernicus portals (e.g. through the CDS Toolbox) will belong to the European Union.

6.3. All other new Intellectual Property Rights created as a result of modifying or adapting the Copernicus information will be owned by the creator.

7. Provision of Third-Party Information and Data
This Licence only covers Copernicus Products. Access to third party products, information, and data related to Copernicus information to which the Licensee is directed or which can be directly accessed through any Copernicus portal will be subject to different licence terms.

8. Disclaimers
8.1. Neither the Licensor nor ECMWF warrant that Copernicus Products will be free from errors or omissions or that such errors or omissions can or will be rectified, or that the Licensee will have uninterrupted, continuous, or timely access to Copernicus Products.

8.2. The Licensor, as well as ECMWF, exclude all warranties, conditions, terms, undertakings, obligations whether express or implied by statute including but not limited to the implied warranties of satisfactory quality and fitness for a particular purpose or otherwise to the fullest extent permitted by law.

9. Liabilities
Neither the Licensor nor ECMWF will accept liability for any damage, loss whether direct, indirect or consequential resulting from the Licensee's use of the Copernicus Products.

10. Termination of and Changes to this Licence

The Licensor may terminate this licence if the Licensee breaches its obligations under these terms. The Licensor may revise this Licence at any time and will notify the Licensee of any revisions.

11. Arbitration Clause and Governing Law
In the event of a dispute arising in connection with this License, the parties shall attempt to settle their differences in an amicable manner. If any dispute cannot be so settled, it shall be settled under the Rules of Arbitration of the International Chamber of Commerce by one arbitrator appointed in accordance with the said rules sitting in London, United Kingdom. The proceedings shall be in the English language. The right of appeal by either party to regular Courts on a question of law arising in the course of any arbitral proceedings or out of an award made in any arbitral proceedings is hereby agreed to be excluded.

It is the intention of the parties that this License shall comprehensively govern the legal relations between the parties to the Licence, without interference or contradiction by any unspecified law. However, where a matter is not specifically covered by these terms or a provision of the Licence terms is ambiguous or unclear, resolution shall be found by reference to the laws of England and Wales, including any relevant law of the European Union.

Nothing stated in this License shall be construed as a waiver of any privileges or immunities of the Licensor or of ECMWF.

Version 1.2 (November 2019)

6.2. Overview on the operational chain

The CAMS Radiation Service operational chain (Fig. 6.1) consists of various parts for handling inputs from several sources, output for the continuous quality control, and output for users.

Satellite-data reception at DLR is performed with two independent antenna systems and a daily rsync is performed to update the rolling archive at DLR. A near-real-time ‘online’ processing chain to generate satellite-based cloud retrievals is operated. As soon as all input satellite raw data is received (i.e. all image segments and all spectral channels) the APOLLO processing is performed at DLR and output is delivered to Transvalor. There is a window up to 60 minutes after the nominal acquisition time – after that the online processing is stopped for the individual satellite image.

Within 1 to 2 days further input data as water vapour, ozone, and aerosol properties from the CAMS global forecast and reanalysis services are obtained. First, they consist of forecasted values, which will be replaced by re-analysis information as soon as this is available.

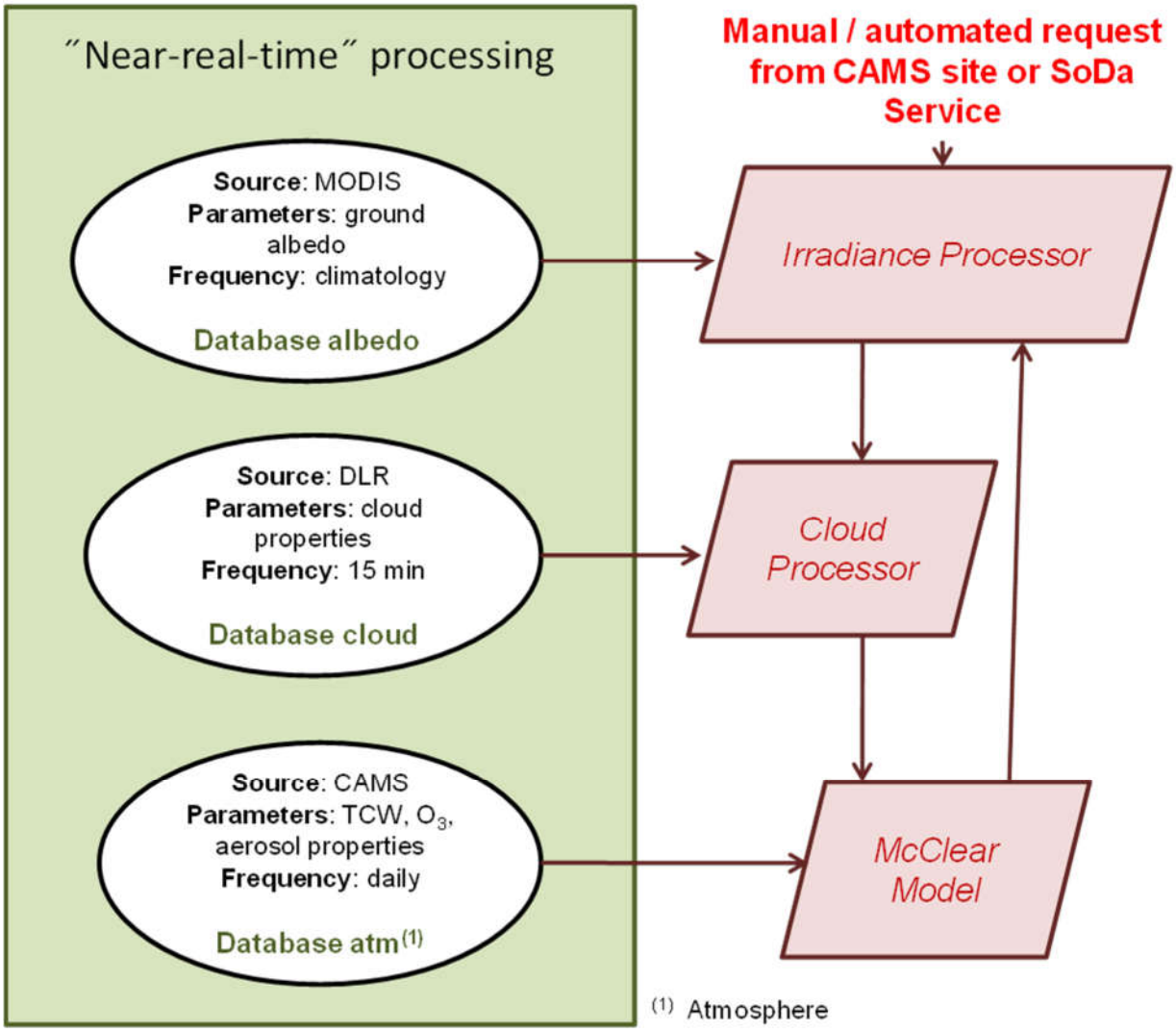

Figure 6.1. Schematic representation of the workflow of the CAMS Radiation Service for computing irradiance products.

Table 6.1. Input data to the CAMS Radiation Service Heliosat-4 method

Variable	Data sources	Temporal resolution	Spatial resolution
Aerosols properties and type	CAMS	3 h	0.8° until 20 June 2016, 0.4° since 21 June 2016
Cloud properties and type	APOLLO/SEV (DLR)	15 min	3 to 10 km
Total column content in ozone	CAMS	3 h	0.8° until 20 June 2016, 0.4° since 21 June 2016
Total column water vapour content	CAMS	3 h	0.8° until 20 June 2016, 0.4° since 21 June 2016
Ground albedo	MINES ParisTech	Climatology of monthly values	6 km

At the end of each calendar month, the 'offline' processing chain for satellite-based cloud retrievals aims at filling gaps in the online processing chain.

McClear service currently uses AOD, ozone and water vapor databases from several sources:

- MACC Reanalysis from 2004 to 2012 (Inness et al., 2013; IFS Cycle 36r1, AODs, ozone and water vapor on a 1.125° grid, approx. 125 km)
- MACC real time analysis from 2013 to 2015 (Morcrette et al., 2009; Benedetti et al., 2009; with updates listed at https://atmosphere.copernicus.eu/changes-cams-global-production-system; ozone and water vapor grid were upgraded to 0.8° (90 km) on 2013-01-01, AOD grid was upgraded to 0.75° (80 km) on 2015-09-03
- CAMS real time analysis since 2016-06-21 (Morcrette et al., 2009; Benedetti et al., 2009; with updates listed at https://atmosphere.copernicus.eu/changes-cams-global-production-system; using IFS Cycle 43r3 or later cycles on a 40 km grid)

All input data are collected in databases at Transvalor premises.

There are two mirror systems of all hardware and processing chains operated at DLR and Transvalor.

For internal quality control purposes, irradiances are calculated routinely at selected locations (see section 6.3).

Publicly available radiation products are time-series of irradiation for a given site and a given period. Once a user request is made via the CAMS Atmosphere Data Store or via scripting, an on-the-fly processing is initiated. It processes the requested time series at the location of interest, the requested duration, and the temporal resolution as requested.

The on-the-fly processing ensures that always the most recent input data and the most recent algorithm version are used. Version numbers are given in the header of each output file and a version history is published at http://solar.atmosphere.copernicus.eu/cams-radiation-service/info. Additionally, the on-the-fly processing allows a smart interpolation of all input data sources to the location of interest.

The majority of users stated time series at the location of their interest as their priority. Nevertheless, two gridded datasets for Europe (http://www.soda-pro.com/de/help/cams-services/cams-radiation-service/download-europe-volume) and Africa (http://www.soda-pro.com/de/help/cams-services/cams-radiation-service/download-africa-volume) in a 0.2° latitude/longitude grid and a 15 min temporal resolution were generated for the period 2005 to 2018.Monthly and yearly average irradiation maps are available for download directly on the web and full resolution gridded datasets can be provided on request.

6.3. Release notes and versioning

Release notes and information on the versioning is available and updated at http://solar.atmosphere.copernicus.eu/cams-radiation-service/info.

6.4. Quality control in the operational processing chain

Several types of quality control are performed in the CAMS Radiation Service workflow:

- checking the smooth running of the product generation workflow in compliance with specifications,
- checking the quality of the inputs to the Heliosat-4 method,
- monitoring the consistency of this quality of product, and detecting possible trends
- checking the smooth running of the service providing the products to users.

Figure 6.2 is a schematic overview of the quality control (this section) and validation procedures (see section 7). The QC / validation procedures both on input and output parameters are given in red.

Inputs to the Heliosat-4 method originate from several sources and have been quality-controlled by their providers. The role of the QC procedures linked to inputs is to detect any gross problem due to transfer and archiving of data and to offer support to the analysis in case of the detection of a possible drawback of the Heliosat-4 method or the CAMS Radiation Service workflow. The procedures are automated and invoked daily.
Input parameters to be controlled for the clear sky model are total aerosol optical depth parameters at 550 and 1240 nm, aerosol optical depth at 550 nm for different species (black carbon, organic matter, dust, sulphate, sea salt, and since 2019 ammonium and nitrate), aerosol type, ozone and water vapour contents. Automatic quality control is performed with respect to completeness of all input products on a daily basis. A dashboard has been set up to perform a visual monitoring of several elements. Figure 6.3 is an example of the automatic monitoring of the collection of data from ECMWF for total column content in

ozone. Besides the completeness of data, also the physical consistency of all input and output parameters needs to be monitored.

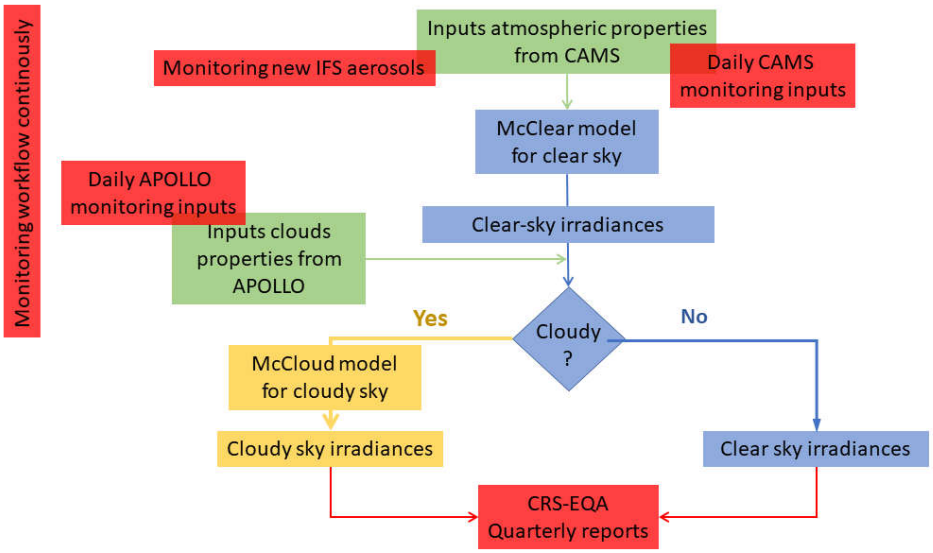

Figure 6.2. Schematic overview of the quality control (QC) and validation procedures

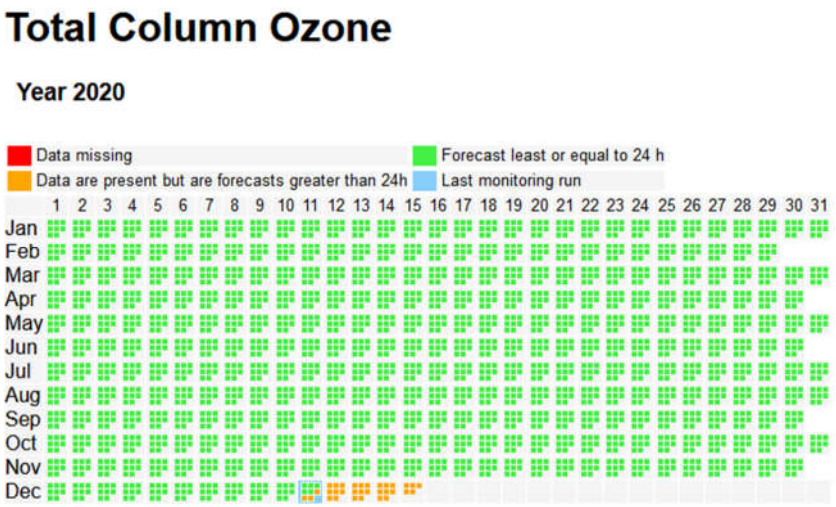

Figure 6.3. Example of the automatically created graph for monitoring the collection of data from ECMWF on total column content in ozone. Each cell (month, day) is made of eight squares, corresponding to the 3 h values.

The position of the Sun in the sky is an important factor in the retrieval of the SSI. The ESRA algorithm in place in the HelioClim-3 and SOLEMI workflows for computing this position has been replaced in the CAMS Radiation Service by the SG2 algorithm (Blanc, Wald 2012) which is much more accurate. Given the number of tests done on this algorithm and its proven accuracy, no ongoing quality control is performed.

The MODIS albedo product MCD43C1 has been treated in order to deliver a database of monthly climatology for the three parameters f_{iso}, f_{vol} and f_{geo} after a fully completion of missing data and time interpolation (Blanc et al., 2014). Thus no automatic control is necessary.

The atmosphere type profile for a geo-point is retrieved from a map based on the cross climate classifications of Köppen-Geiger and Trewartha as explained in Lefevre et al. (2013). Thus no automatic control is necessary.

The monitoring of input data for Heliosat-4 was changed during 2017. The previously used monitoring was designed to detect unusual variations of the CAMS radiation service input parameters. It consisted of statistical distributions of 1 min for rolling periods (5 days from day d-2, or 30 days from d-2) of each parameter compared to a reference. This reference was the statistical distribution of the same period, but for the years 2013-2016. These statistical distributions were represented as boxplots, and an alarm is set to detect unusual variations. In order to make this alarm useful, it was supposed to observe stable climatological zones, for example the desert of Mauritania which consists in an amount of about 30 pixels between latitudes (+20°, +24°) and longitudes (-7°, -2°).

Due to the change of a new ECMWF/IFS version with higher spatial resolution, the concept of stable areas is not appropriate any more. The statistical distribution is sensitive to changes in spatial resolution and may be sensitive to major IFS changes in future. Given this context, the previous consistency monitoring was replaced by two types of monitoring:

i. A daily visual monitoring of daily means of AOD, global, diffuse and direct radiations from CAMS with a time-series of rolling 30 days.

ii. A monitoring of the impact of new IFS aerosols on a study basis when necessary. These reports are available as well.

6.4.1. Daily monitoring of input parameters

This activity aims at verifying the smooth running of the service, as well as the consistency of the data during the period.
It consists of a daily visual monitoring of daily means of type-wise AOD, cloud coverage (COV), cloud type (CT), cloud optical depth (COD), ozone (O3), water vapour (WV), global, diffuse and direct radiations from CAMS with a time-series of rolling 30 days from real time minus two days. BSRN stations of Carpentras (France) and Camborne (U.K.) as well as a Pirata station at 0°N 23°W (Atlantic) are used. Once computed, the time-series can be visualized on a webpage, and a mail is sent in order to notify the success or the failure of the procedure. As an example, Figure 6.4 presents the graphs edited daily for Carpentras.

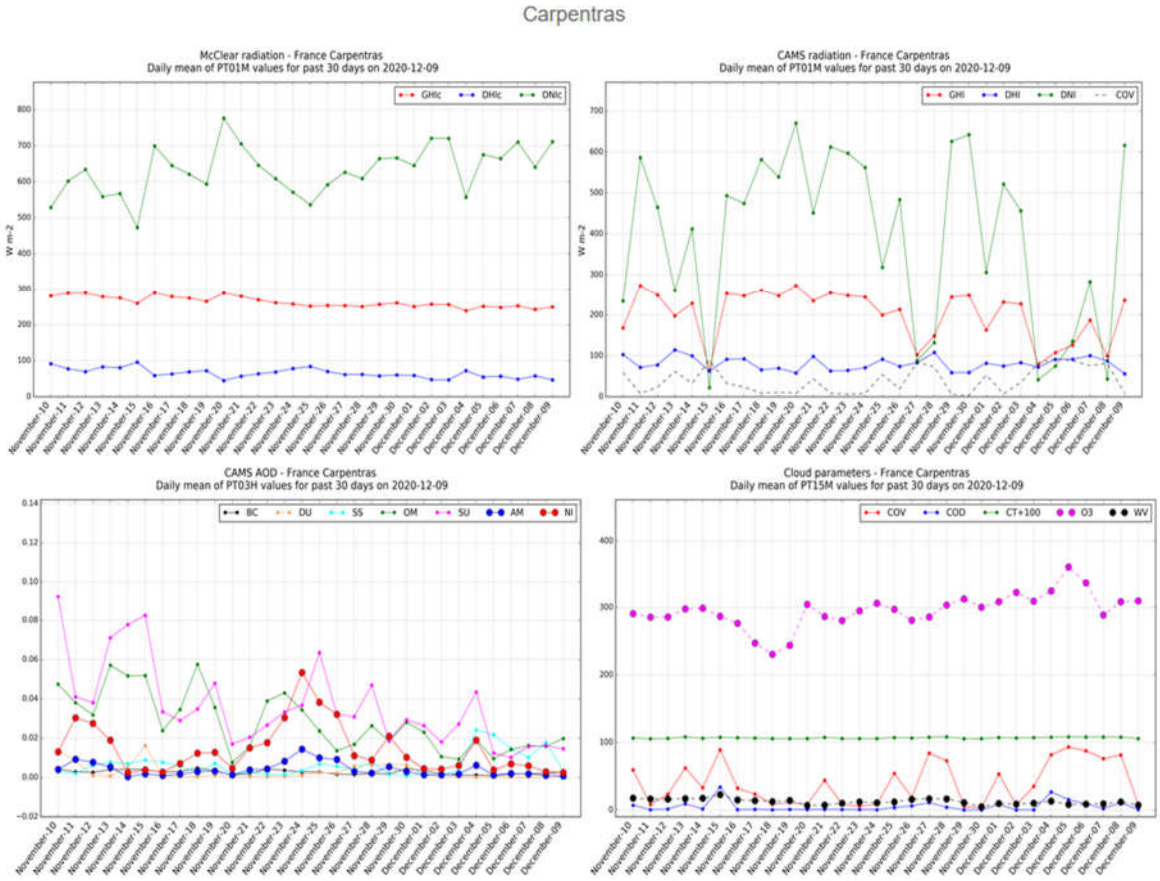

Figure 6.4. Example - daily monitoring graphs edited for station Carpentras.

6.4.2. Monitoring IFS cycles

A monitoring of the impact of new IFS aerosols is regularly done. Comparisons are done between the CAMS DNI product and ground measurements for a few stations and between the operational (o-suite) and the experimental (e-suite) datasets. These results are further illustrated with 2D histograms between ground measurements and the CRS products, with histograms of their deviations, with histograms of their values, and with their monthly means and standard-deviations (cf. deliverable CAMS72_2018SC1 – CAMS monitoring IFS cycle update report, Nov. 2019 and future, similar reports).

6.5. Standard output mode products

There are two groups of radiation products (Tab 6.3 and 6.4) in the CAMS Radiation Service:

- CAMS Clear-Sky Radiation (McClear) products:
  These products describe the clear-sky SSI for the whole world, starting from 2004 and on-going. This product is the result of a numerical atmospheric composition model together with a radiative transfer model and is not based on the processing of Meteosat data.

- CAMS All-Sky Radiation (Heliosat-4) products:
  This series describes all skies (cloudy or not) SSI within the MSG field of view, starting from 2004 and on-going.

Table 6.3. Definition of the surface solar downward irradiation (SSI) parameters contained in the products

Acronym	Definition
GHI	All-sky global irradiation, i.e., the SSI integrated over the whole spectrum available at ground level, on a horizontal surface
DifHI	All-sky diffuse irradiation, i.e., the diffuse part of the SSI integrated over the whole spectrum available at ground level, on a horizontal surface
DirHI	All-sky direct (beam) irradiation, i.e., the direct part of the SSI integrated over the whole spectrum available at ground level, on a horizontal surface
DNI	All-sky Direct Normal Irradiation. Part of the radiation that is received from the direction of the sun by a plane facing the sun.

Table 6.4. Main features of the standard output products

	CAMS Clear-Sky (McClear)	CAMS All-Sky (Heliosat-4)
Type of product	time-series	
Parameters	GHI, DifHI, DirHI, DNI	
Geographical area	global	Europe / Africa / Middle East / Atlantic Ocean (MSG field of view, please note restrictions as described in section 5.4 on satellite viewing angles larger than 60°)
Horizontal resolution	interpolated to point of interest	
Time coverage	from 2004-01-01 to (current – 2 days)	from 2004-02-01 to (current – 2 days)
Temporal resolution	1 min, 15 min, 1 h, 1 day, 1 month	
Data format	ASCII (CSV), NetCDF HDF (via script access only)	
Data file size	File size is depending on the temporal resolution. Largest files are in 1 min temporal resolution and the csv data format (e.g. 60 MB for a 1 year time series in the standard output mode and 10 MB if zipped; 138 MB for a 1 year time series in the expert mode and 19 MB if zipped)	

Data access	CAMS Atmosphere Data Store
Processing	on request within a few minutes
Update of the databases	2 days delayed mode

The period of integration is defined as the time during which the solar radiation is integrated to yield a period-sum. For example, an integration period of 1 h means that the delivered irradiation is the hourly sum of 1 min irradiation values during one hour. Following meteorological standards, the time given for an irradiation value is the end of the integration period. For example, the value given for 11:00 means an integration period from 10:00:01 to 11:00:00 if the period is 1 h, or 10:30:01 to 11:00:00 if the period is 30 min.

A gap handling is performed automatically since the update on 20 June 2018. It is applying the following principles:

- The CAMS Radiation Service provides NaN values if large gaps (larger than 1 day) of missing satellite input data exist.

- Shorter gaps of less than a day during daytime are filled with linearly interpolated k_c and k_{cB}. These cases are marked with reliability = 0. These cases mainly occur due to missing satellite raw data.

- In low sun conditions APOLLO does not provide any cloud detection and cloud optical depth. Therefore, the first available k_c value is kept constant for the time between sunrise and this point in time. The same is done in the evening hours – the last available k_c value is kept constant until sunset.

- The reliability index is computed with respect to the amount of 1 minute resolution time slots of the current time summarization (e.g. 15 min or 1 hour) without available cloud information. So, it provides the information how many interpolated cloud time instants are used in the summarization interval.

6.6. Detailed info expert output mode

For expert users, all input and output parameters are provided in the 'detailed info expert output mode'. It can be selected when requesting 1 min resolved time series. Besides the standard outputs, it provides (as from 3 July 2019 onwards):

- Irradiation on horizontal plane at the top of atmosphere
- Clear sky irradiation values
    - Clear sky GHI. Clear sky global irradiation on horizontal plane at ground level
    - Clear sky BHI. Clear sky beam irradiation on horizontal plane at ground level

    - Clear sky DHI. Clear sky diffuse irradiation on horizontal plane at ground level (Wh/m2)
    - Clear sky BNI. Clear sky beam irradiation on mobile plane following the sun at normal incidence
- All sky irradiation values
    - All sky GHI. Clear sky global irradiation on horizontal plane at ground level
    - All sky BHI. Clear sky beam irradiation on horizontal plane at ground level
    - All sky DHI. Clear sky diffuse irradiation on horizontal plane at ground level
    - All sky BNI. Clear sky beam irradiation on mobile plane following the sun at normal incidence
- Solar zenithal angle for the middle of the summarization (deg)
- Atmospheric profile code: afglus=U.S. standard afglt=tropical afglms=midlatitude summer afglmw=midlatitude winter afglss=subarctic summer afglsw=subarctic winter
- Total column content of ozone (Dobson unit)
- Total column content of water vapour (kg/m2)
- AOD BC. Partial aerosol optical depth at 550 nm for black carbon
- AOD DU. Partial aerosol optical depth at 550 nm for dust
- AOD SS. Partial aerosol optical depth at 550 nm for sea salt
- AOD OR. Partial aerosol optical depth at 550 nm for organic matter
- AOD SU. Partial aerosol optical depth at 550 nm for sulphate
- AOD NI. Partial aerosol optical depth at 550 nm for nitrate. This quantity was introduced in July 2019 and will have zero values before – indicating unavailability.
- AOD AM. Partial aerosol optical depth at 550 nm for ammonium. This quantity was introduced in July 2019 and will have zero values before – indicating unavailability.
- Deprecated and replaced by AOD NI: AOD 550. Aerosol optical depth at 550 nm
- Deprecated and replaced by AOD AM: AOD 1240. Aerosol optical depth at 1240 nm
- Deprecated, but kept for format consistency: alpha Angstroem coefficient for aerosol. It is set to zero values.
- Deprecated, but kept for format consistency: Aerosol type. Type of aerosol: -1=no value 5=urban 7=continental clean 8=continental polluted 9=continental average 10=maritime clean 11= maritime polluted 12=maritime tropical 13=antarctic 14=desert
- fiso. MODIS-like BRDF parameter fiso

- fvol. MODIS-like BRDF parameter fvol
- fgeo. MODIS-like BRDF parameter fgeo
- albedo. Ground albedo
- Cloud optical depth (value of the nearest acquisition time of the pixel, not interpolated over time)
- Cloud coverage of the pixel (percentage from 0 to 100, value of the nearest acquisition time of the pixel, not interpolated over time)
- Cloud type (value of the nearest acquisition time of the pixel, not interpolated over time) -1=no value 0=no clouds 5=low-level cloud 6=medium-level cloud 7=high-level cloud 8=thin cloud
- non-bias corrected all-sky radiation values
    - non-corrected all sky GHI. Clear sky global irradiation on horizontal plane at ground level
    - non-corrected all sky BHI. Clear sky beam irradiation on horizontal plane at ground level
    - non-corrected all sky DHI. Clear sky diffuse irradiation on horizontal plane at ground level
    - non-corrected all sky BNI. Clear sky beam irradiation on mobile plane following the sun at normal incidence

Users may

- make use of this information to establish an extended bias correction based on own localized ground observations;
- use this transparency about all input parameters to run their own solar radiation retrieval schemes;
- contribute easily to evaluation and method development of Heliosat-4 by having access to all input variables;
- develop downstream services by making use on the knowledge on all input parameters e.g. in artificial intelligence methods.

Note should be taken that the content of the detailed info mode may change depending on the version of Heliosat-4 or McClear. Each product contains a detailed description of its content and the user should refer to it.

6.7. How to make a request for a CAMS Radiation Service product

The CAMS catalogue is available at https://atmosphere.copernicus.eu/catalogue#/. Browsing for ‘Solar Radiation’ provides interactive access to the services on clear-sky and all-sky irradiation in a web-based graphical user interface. Furthermore, the new Atmosphere Data Store offers access to the CAMS Radiation Service at https://ads.atmosphere.copernicus.eu.

The CAMS Radiation Service is making use of the infrastructure being developed and provided by the SoDa Service (www.soda-pro.com) which is well-known in the solar radiation community which uses it intensively (section 6.9). The CAMS Atmosphere Data Store is available at https://ads.atmosphere.copernicus.eu. The 'Solar Radiation time series' provides access to a description of the data set, a form to download the data, and to the documentation and quality control information. The Download data tab provides a simple form to access the services on clear-sky and all-sky irradiation.

Requests are made through an information system (section 6.8). The CAMS Radiation Service is making use of the infrastructure being developed and provided by the SoDa Service (www.soda-pro.com) which is well-known in the solar radiation community which uses it intensively.

To ensure service stability and avoid misuse, a maximum number of time series requests per day and per user is implemented. The number of users reaching this limit is monitored automatically. In case of too many rejected user requests, the hardware will be enhanced.

Users needing a large number of time series may contact the CAMS help desk and get additional support.

Users need to register for the Atmosphere Data Store with an email and a password. They need to accept the CAMS data policy (section 6.1).

The inputs by users needed to trigger a request for a selected CAMS Radiation Service product are:

- cloud-free conditions only or both cloud-free and actual weather conditions
- the geographical coordinates of the site of interest,
- the elevation of this site above sea-level. By default, the application uses well-known digital elevation models, such as NASA-SRTM,
- the period of time: begin data, end date,
- the summarization, i.e. the period of integration of the SSI, e.g. hourly irradiation.
- time reference
- format

There are two options to perform a data request – either interactively via the CAMS Atmosphere Data Store or via a API request. An example API request can be generated using the online form.

6.8. Format of products

6.8.1. Data formats

Three formats are provided: CSV (comma-separated values), binary NetCDF and binary HDF formats. Note that the HDF format is only available in the script access mode.

The CSV format is a human-readable format, more exactly an ASCII format. Each value is separated from the others by a comma or a semi-column. It can be easily ingested by tools such as Microsoft or OpenOffice suites, Matlab or proprietary applications written in any language (e.g., C, PHP, Python…).

In order to follow changes in technology, the NetCDF format has been adopted. NetCDF is a set of software libraries and self-describing, machine-independent data formats that support the creation, access, and sharing of array-oriented scientific data. NetCDF was developed and is maintained at Unidata, part of the University Corporation for Atmospheric Research (UCAR) Community Programs (UCP) in USA. Unidata is funded primarily by the National Science Foundation of USA. It is one of the formats recommended by the GEOSS (Global Earth Observation System of Systems) programme to which is contributing GMES / Copernicus. Several tools are available in the NetCDF Web site to create, handle and exploit NetCDF files (www.unidata.ucar.edu/software/netcdf/).

6.8.2. Metadata

Metadata are available to describe the CAMS Radiation Service products in GEOSS-compliant portals. These are *discovery* metadata that permit the cataloguing of these products and therefore to users to discover the products. These metadata obey to INSPIRE implementation rules (Ménard et al., 2009). As an example the structure of the CSV files is described – the NetCDF implementation is technically of course different, but the meaning of metadata remains the same.

The CAMS Radiation Service CSV formatted products are organised as lines of values (columns). Before the first line of data, there is a set of metadata for exploitation of the data. These metadata are written as text in the delivered file. They obey the ISO standard when available. They describe what are the various elements contained in a product. Currently these metadata are:

- *title*: title of the time-series, e.g., “CAMS Radiation Service v3.2 all-sky irradiation (derived from satellite data)”,
- *content*: a short description of the content of the product, e.g., “A time-series of solar radiation received on horizontal plane and plane always normal to the sun rays at ground level.”,
- *provider*: name of the provider, e.g., “MINES ParisTech (France)”,
- *date begin, date end*: dates of the beginning and end of the period. The date follows the ISO 8601 standard, e.g. 2004-01-01T01:00:00.000.

- *site latitude and longitude*: geographical coordinates of the site, positive North and positive Earth. The ISO 19115 standard is used,
- *elevation*: elevation above sea level in m,
- *time reference*: time system used: Universal Time (UT), or True Solar Time (TST). This metadata is present only when the period of integration is less than 1 day,
- *summarization*: period during which the energy is summed up to obtain a power average, e.g., 15 min,
- *sampling rate*: period with which the resulting irradiation is sampled. Usually, the sampling rate is set equal to *summarization*,
- *noValue*: the code denoting the absence of value, e.g. NaN (not a number).

The content of each column is described as a free text.
Each line corresponds to an instant of observation. The typical content of a line is:

- instant of observation,
- irradiation at the top of the atmosphere,
- clear-sky irradiation value at ground level, e.g. Clear Sky GHI
- all-sky irradiation value at ground level, e.g., GHI,
- reliability code, ranging from 0 to 1.

The exact content of a line depends on the type of product and this is why metadata are included in the file.

Fig. 6.5 provides an example of the typical standard output mode file header. Additionally, there is the detailed info output mode (section 6.6) providing an extended output (Fig. 6.6).

```
# Coding: utf-8
# File format version: 2
# Title: CAMS Radiation Service v3.2 all-sky irradiation (derived from satellite data).
# Content:  A time-series of solar radiation received on horizontal plane and plane always normal to the sun rays at ground level.
#         Returns the global, beam and diffuse irradiations integrated over a selected time step,
#         for a selected location (Meteosat Second Generation satellite coverage) and a selected period.
# The research leading to these results has received funding from the European Union within the Copernicus programme.
# Provider: MINES ParisTech (France)
# More information at: http://www.soda-pro.com/web-services/radiation/cams-radiation-service
# Date begin (ISO 8601): 2004-02-01T00:00:00.0
# Date end (ISO 8601): 2004-02-03T00:00:00.0
# Latitude (positive North, ISO 19115): 22.5561
# Longitude (positive East, ISO 19115): 13.6289
# Altitude (m): 709.00
# Time reference: Universal time (UT)
#
# Encoding partly from D2.8.III.13-14 INSPIRE Data Specification on Atmospheric Conditions and Meteorological Geographical Features - Technical Guidelines (2013-12-10) and CF (Climate and Forecast) metadata (2013-11-11)
# CF Standard Names registry of ObservablePropertyValue
# http://cfconventions.org/Data/cf-standard-names/27/build/cf-standard-name-table.html
# urn:x-inspire:specification:DS-AC-MF:observable-property-name:cf-standard-name:1.6
# ObservableProperty
#    basePhenomenon:"integral_of_surface_downwelling_shortwave_flux_in_air_sky_wrt_time"
#    uom:"Wh m-2" [unit]
# StatisticalMeasure
#    statisticalFunction: "sum"
# Summarization (integration) period: 0 year 0 month 0 day 0 h 1 min 0 s
# noValue: nan
#
# Columns:
# 1. Observation period (ISO 8601)
# 2. TOA. Irradiation on horizontal plane at the top of atmosphere (Wh/m2)
# 3. Clear sky GHI. Clear sky global irradiation on horizontal plane at ground level (Wh/m2)
# 4. Clear sky BHI. Clear sky beam irradiation on horizontal plane at ground level (Wh/m2)
# 5. Clear sky DHI. Clear sky diffuse irradiation on horizontal plane at ground level (Wh/m2)
# 6. Clear sky BNI. Clear sky beam irradiation on mobile plane following the sun at normal incidence (Wh/m2)
# 7. GHI. Global irradiation on horizontal plane at ground level (Wh/m2)
# 8. BHI. Beam irradiation on horizontal plane at ground level (Wh/m2)
```

```
# 9. DHI. Diffuse irradiation on horizontal plane at ground level (Wh/m2)
#10. BNI. Beam irradiation on mobile plane following the sun at normal incidence (Wh/m2)
#11. Reliability. Proportion of reliable data in the summarization (0-1)
#
# Observation period;TOA;Clear sky GHI;Clear sky BHI;Clear sky DHI;Clear sky
BNI;GHI;BHI;DHI;BNI;Reliability
2004-02-01T00:00:00.0/2004-02-
01T00:01:00.0;0.0000;0.0000;0.0000;0.0000;0.0000;0.0000;0.0000;0.0000;0.0000;1.0000
2004-02-01T00:01:00.0/2004-02-
01T00:02:00.0;0.0000;0.0000;0.0000;0.0000;0.0000;0.0000;0.0000;0.0000;0.0000;1.0000
```

Figure 6.5 Header of the times-series edited as provided by the CAMS Radiation Service in the standard output mode. In this example the time step is 1 min. Columns are the same for 15 min, 1 h, 1 day, and 1 month summarizations.

Columns:
1. Observation period (ISO 8601)
2. TOA. Irradiation on horizontal plane at the top of atmosphere (Wh/m2)
3. Clear sky GHI. Clear sky global irradiation on horizontal plane at ground level (Wh/m2)
4. Clear sky BHI. Clear sky beam irradiation on horizontal plane at ground level (Wh/m2)
5. Clear sky DHI. Clear sky diffuse irradiation on horizontal plane at ground level (Wh/m2)
6. Clear sky BNI. Clear sky beam irradiation on mobile plane following the sun at normal incidence (Wh/m2)
7. GHI. Global irradiation on horizontal plane at ground level (Wh/m2)
8. BHI. Beam irradiation on horizontal plane at ground level (Wh/m2)
9. DHI. Diffuse irradiation on horizontal plane at ground level (Wh/m2)
#10. BNI. Beam irradiation on mobile plane following the sun at normal incidence (Wh/m2)
#11. Reliability. Proportion of reliable data in the summarization (0-1)
#12. sza. Solar zenithal angle for the middle of the summarization (deg)
#13. atm. Atmospheric profile code: afglus=U.S. standard afglt=tropical afglms=midlatitude summer afglmw=midlatitude winter afglss=subarctic summer afglsw=subarctic winter
#14. tco3. Total column content of ozone (Dobson unit)
#15. tcwv. Total column content of water vapour (kg/m2)
#16. AOD BC. Partial aerosol optical depth at 550 nm for black carbon
#17. AOD DU. Partial aerosol optical depth at 550 nm for dust
#18. AOD SS. Partial aerosol optical depth at 550 nm for sea salt
#19. AOD OR. Partial aerosol optical depth at 550 nm for organic matter
#20. AOD SU. Partial aerosol optical depth at 550 nm for sulphate
#21. AOD NI. Partial aerosol optical depth at 550 nm for nitrate
#22. AOD AM. Partial aerosol optical depth at 550 nm for ammonium
#23. alpha. Angstroem coefficient for aerosol
#24. Deprecated, but kept for format consistency: Aerosol type. Type of aerosol: -1=no value 5=urban 7=continental clean 8=continental polluted 9=continental average 10=maritime clean 11= maritime polluted 12=maritime tropical 13=antarctic 14=desert
#25. fiso. MODIS-like BRDF parameter fiso
#26. fvol. MODIS-like BRDF parameter fvol
#27. fgeo. MODIS-like BRDF parameter fgeo
#28. albedo. Ground albedo
#29. Cloud optical depth (value of the nearest acquisition time of the pixel)
#30. Cloud coverage of the pixel (percentage from 0 to 100, value of the nearest acquisition time of the pixel)
#31. Cloud type (value of the nearest acquisition time of the pixel) -1=no value 0=no clouds 5=low-level cloud 6=medium-level cloud 7=high-level cloud 8=thin cloud
#32. GHI no corr. Global irradiation without bias correction on horizontal plane at ground level (Wh/m2)
#33. BHI no corr. Beam irradiation without bias correction on horizontal plane at ground level (Wh/m2)
#34. DHI no corr. Diffuse irradiation without bias correction on horizontal plane at ground level (Wh/m2)
#35. BNI no corr. Beam irradiation without bias correction on mobile plane following the sun at normal incidence (Wh/m2)

Figure 6.6 Legend of the parameter columns in the detailed info mode of 1 min CAMS Radiation Service All-Sky times-series.

6.9. Description of the CAMS Radiation Service Information System

Given the experience gained by several precursor services delivering databases and applications relating to solar radiation, the CAMS Radiation Service Information System has been designed as a series of Web services that disseminate the products.

These Web services follow the GEOSS (Global Earth Observation System of Systems) standards for interoperability and therefore can be exploited by any GEOSS-compliant portal. This ensures a wide dissemination, more efficient than establishing a specific Web site.

In more details, the system is based on the technologies recommended by the EU-funded MESoR project, the International Energy Agency Task SHC 36, and the GEOSS AIP projects, in order to reduce the amount of technological development and to benefit from the adopted standards. The basic concept is the following:

- products from the CAMS Radiation Service can be accessed through the CAMS Atmosphere Data Store,
- each CAMS Radiation Service Web service is an application that can be invoked through the Web using GEOSS standards,
- the CAMS Radiation Service Web services are deployed on the energy community portal (webservice-energy.org) from which they can be executed,
- the CAMS Radiation Service Web services are described in existing catalogues to increase their visibility,
- the CAMS Radiation Service Web services bear clear references and link to the CAMS Radiation Service and the Copernicus Atmospheric Service (CAMS) as a whole,
- invoking a CAMS Radiation Service Web service can be done only if the user is a registered user in the database of users of the CAMS Radiation Service and has signed the Licence terms for CAMS Products and Services,
- benefit from the interoperability capability of the CAMS Radiation Service Web services in order to increase their visibility. In particular,
    - expose the CAMS Radiation Service Web services in the catalogue of the CAMS Atmosphere Data Store
    - expose the CAMS Radiation Service Web services on the collaborative SoDa Service, built on the most advanced Web technologies and free software. One of the advantages is to benefit from the large penetration rate of the current SoDa Service in the solar energy community
    - expose the CAMS Radiation Service Web services in GEOSS-compliant catalogues
    - allow the exploitation of the CAMS Radiation Service Web services by any other portal or application under certain conditions.

6.9.1. The CAMS Radiation Service Information System as a GEOSS component

Figure 6.7 depicts the infrastructure and its integration as a GEOSS component. The CAMS Radiation Service operational system and the corresponding radiation database are represented by a box on the right of the graph. Users may request for time-series of radiation values from a web site, shown on the left. In this example, the SoDa Service is shown and is one of many possible clients. It hosts a client: the CAMS Radiation Service Client, which is the interface to the users, collects inputs for time-series, such as location and period, and delivers time-series. The SoDa Service does not connect directly to the CAMS Radiation Service application. An intermediate has been set-up in order to ensure interoperability and facilitate exploitation of CAMS Radiation Service results by other clients. This intermediate is a Web service, more exactly a Web Processing Service (middle of the figure). It receives the request from the CAMS Radiation Service Client, makes itself queries to the CAMS Radiation Service operational system, and flows the resulting time-series to the client.

To ensure a wide dissemination, the CAMS Radiation Service information system is declared as a GEOSS component by registering the component Web Service in a thematic catalogue on energy, itself registered in the GEOSS Components and Services Registry (GEOSS CSR box in the lower right part in Figure). By this means, anyone may discover the CAMS Radiation Service Web Service and will be supplied with details on how to exploit them as discussed in the next section.

Invocation of the CAMS Radiation Service Web Service is done by the means of a client, called CAMS Radiation Service client in the Figure. This client is provided by the CAMS Radiation Service team or may be developed on the user side as well.

The website webservice-energy.org is a GEOSS community portal. It is an initiative of MINES ParisTech / Armines to host web services dedicated to solar radiation and more generally, energy. The website has several web services: Web Map Services, Web Processing Services, obeying OGC (Open Geospatial Consortium) or W3C (World Wide Web Consortium) standards. The W3C standard is abandoned in favour of the OGC standard. Several services have been developed by MINES ParisTech, others by other providers such as DLR.

The website comprises also a catalogue obeying the OGC CSW (Catalogue Service for the Web) standard. The open-source Geonetwork (geonetwork-opensource.org) has been adopted as a CSW tool. Resources are described via metadata that are INSPIRE-compliant (INSPIRE: Infrastructure for Spatial Information in Europe). The catalogue describes the CAMS Radiation Service service, thus enabling its discovery and further exploitation. The catalogue is registered in the GEOSS Components and Services Registry; this ensures that the catalogue is fully aligned with GEOSS standard and increases the chances of discovery of the components registered in the catalogue.

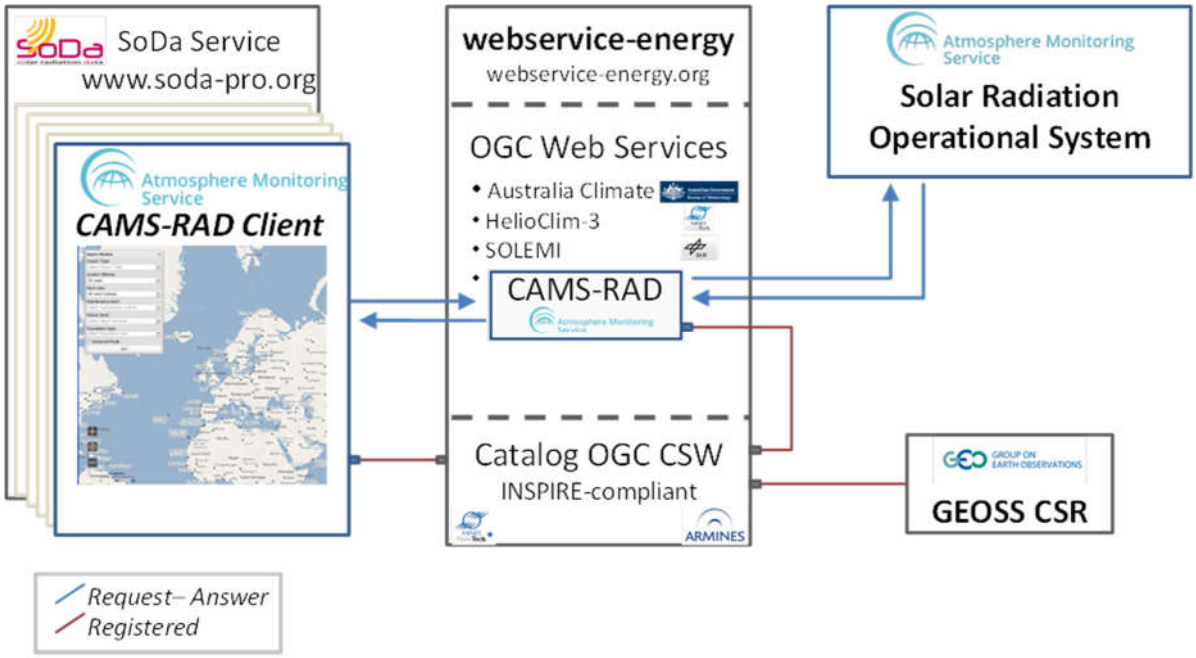

Figure 6.7. Sketch of the CAMS Radiation Service Information System and its integration as a GEOSS component

6.9.2. Web Processing Service (WPS)

Accessing the CAMS Radiation Service product is done by the means of a Web Processing Service which obeys the standard set up by the OGC and recommended by GEOSS.

The OpenGIS® Web Processing Service (WPS) Interface Standard provides rules for standardizing inputs and outputs (requests and responses) for services aimed at processing the geospatial information extracted from the geographic databases. Here, the CAMS Radiation Service service is defined for the Meteosat field-of-view and the “processing” is the extraction of a time-series for a given location, given period, and summarization.

The standard also defines how a client can request the execution of a process, and how the output from the process is handled. It defines an interface that facilitates the publishing of geospatial processes, their discovery by clients and the linking to those remotely hosted processes. The data required by the WPS can be delivered across a network or can be available through the local server.

WPS defines three operations, two describing service metadata and Input/Output (I/O) characteristics, and a third to execute/run the process:

- getCapabilities: generic WPS instance metadata, list of services in instance,
- describeProcess: full description I/O of service,
- execute: process execution with provided inputs and returned a formatted output, i.e. a netCDF file.

There are several frameworks available to develop and deploy OGC Web Processing Services. Two have been selected configurable application that are released under GNU General Public Licence (GPL) and facilitate the conversion of applications into a Web Processing Service (WPS) in OGC standards. One is the “Toolbox” from the company INTECS, developed in the progress of the Integrated Project (2008-2011) GENESIS funded by the European Commission DG-INFSO under the 7th Framework Programme. The other tool is PyWPS, an open-source project managed by the company Intevation. On the front end, the PyWPS or Toolbox encodes the outputs of the WPS using SOAP and transfers it using HTTP. On the back end, it can be connected via shell scripts to the application, here the CAMS Radiation Service service.

There are two WPS: One is the CAMS Clear-Sky/McClear Radiation service that provides time-series of the SSI that would be observed at any place in the world any time if the sky were clear starting from 2004-01-01. The second WPS is the CAMS Total-Sky Radiation Service that provides time-series of the SSI received at any place in the field-of-view of the Meteosat satellites any time starting from 2004-02-01.

6.9.3. The CAMS Radiation Service clients

A client is the interface between users and a WPS. Several frameworks can be used to develop such a client. In the course of the MACC-II and MACC-III projects, two clients have been developed in close collaboration with Transvalor for the SoDa Service, acting as a broker in the collaborative system.

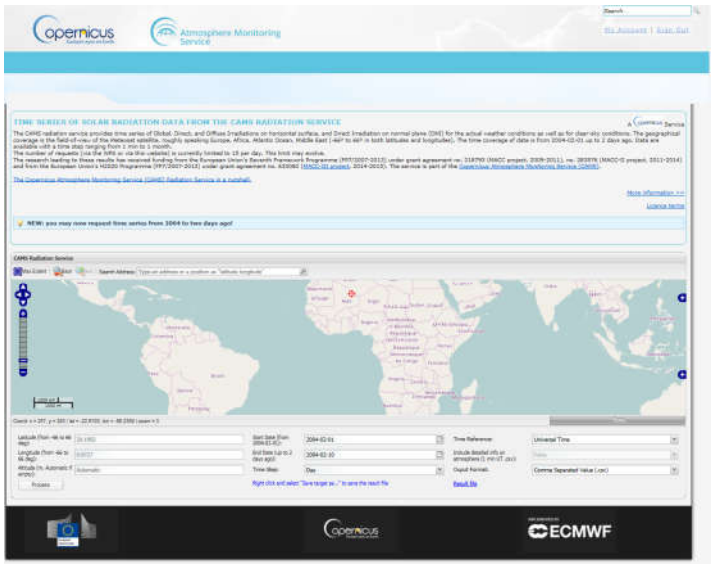

Figure 6.8. Interface of the CAMS Radiation Service client in the SoDa Service. The result is a file that can be saved or displayed. The format of the result file is either CSV (comma-separated values) or NetCDF

One client is for CAMS Radiation Service Clear-Sky/McClear and the second one for CAMS Radiation Service Total-Sky product. Figure 6.8 is a screenshot of the CAMS Radiation Service

Total-Sky client. This client permits to invoke the CAMS Radiation Service WPS. It can also be launched from the CAMS Web site and the CAMS catalogue.

The client is not necessarily an interface for human use. Several registered users of the CAMS Radiation Services have developed applications that invoke in an automated manner the WPS, get the outcomes and exploit them.

7. Validation

7.1. Principles and limitations

The usual way of assessing the quality of retrievals of SSI derived from satellite images is to compare these SSI to coincident measurements performed at ground level. The typical relative accuracy of good quality measurements of the global SSI in the global meteorological network is 4% in terms of root mean square error (WMO, 2012). Therefore, the ground measurements can be seen as an accurate reference against which one may compare the SSI derived from satellite. The comparison is made by computing the difference between the two sets of measurements and analysing statistical quantities such as the bias or the root mean square error.

However, the actual situation is not that simple. Several limitations exist that make the assessment of the quality of retrieved irradiances a very difficult task.

The first limitation is the quality of the ground measurements. Well-maintained stations are rare. Data are often questionable. They should undergo extensive procedures for checking quality. Such procedures are often not enough and a final check must be performed by a trained meteorologist to discard suspicious data. For example, a series of ground-measured data sets was produced during the MESoR project[2], to serve as a reference for the benchmarking of any solar radiation product device from satellite data (Hoyer-Klick et al., 2008).

Even in case of accurate measurements, one often encounters a problem of time system. The time system for acquisition may be universal time, mean solar time, true solar time or local time. However, when stored in a database, there is a conversion in another time system, e.g., universal time. There is consequently a change of original values due to a resampling in time. This resampling can be done using various techniques, usually unspecified. In any case, it is not possible to return to the original values and there is a systematic shift of a fraction of an hour between the two sets of measurements. This leads to an additional difference.

Moreover, the networks do not always follow the existing standard for defining hourly data. This standard is defined by the WMO (WMO 1981): the time assigned to a data corresponds to the end of the measurement period. For example, hourly data assigned to 11:00 UT has been measured between 10:00 and 11:00 UT. In several cases, the time associated to a measurement represents the beginning of the period, or the middle of the period, or any instant within the period. Again, the comparison between the two sets requires the resampling of one of the sets at the expenses of decay in quality.

2 Project MESoR (Management and Exploitation of Solar Resource Knowledge) funded by the European Commission, from 2007 to 2009 , http://www.mesor.org/

The limitations expressed above due to the time do not hold if one deals with daily, monthly or yearly averages or sums of SSI.

A severe limitation is due to the large differences in principles of measurements. Single point and temporally integrated data (ground measurements) are compared to spatially integrated and instantaneous data (satellite estimates). An assumption of ergodicity (e.g. here equivalence between the temporal and spatial averages) is usually made. This assumption is correct only if the field is spatially homogeneous over an area much larger than a pixel. This is generally false when a significant physiographic feature is present. Other local effects such as reflections on the surrounding slopes or the shadows of clouds may add to the difficulty in comparison.

Perez et al. (1997), Zelenka et al. (1999) have observed the local variability of the SSI using measurements made by well-calibrated ground stations close to each other. They found that the variability itself is highly variable from one region to another. Nevertheless, they demonstrate that this variability cannot be ignored. Expressing this variability as the ratio of the variance relative to the mean value over the area, they found typical variability in hourly irradiances of 17 % for an area of 10 km in radius. This means that within a 10 x 10 km² area, irradiances measured by a series of similar inter-calibrated sensors would exhibit the same mean value but would differ from hour-to-hour, with a relative variance equal to 17 %. Therefore, observing a relative difference hour-to-hour of 17% between a single pyranometer located in a pixel cannot mean that the satellite-derived irradiances are of bad quality.

The relative variability increases as the surface of the area increases. For example, it typically reaches 25% for a radius of 30 km. It decreases as the time integration increases. For example, it is down to 10% for daily values and a radius of 10 km.

Zelenka et al. (1999) analysed the actual accuracy of satellite estimations of hourly SSI. They suggest that for a relative deviation of 23% (root mean square error) between ground measurements and satellite estimations, only half of it is due to the estimation method itself. The difference comes from:

- error on the measurements provided by the pyranometer (3 to 5%);
- error due to the spatial variability of solar radiation within the pixel (5 to 8%)
- error due to spatial and temporal heterogeneity of the compared data, e.g. assuming ergodicity (3 to 5%) as discussed above.

7.2. Overview of the validation activities

Outcomes of the CAMS Radiation Service have to be validated on a periodic basis. Following practices in CAMS, this validation is performed every quarter year. Following current

practices in assessment of satellite-derived data in solar energy, the irradiances provided by the CAMS Radiation Service are tested against qualified ground measurements measured in several ground-based stations serving as reference. These ground measurements are coincident in time with the CAMS Radiation Service estimates.

The CAMS Radiation Service maintains a catalogue of stations providing ground measurements suitable for the validation. This catalogue is updated at least once a year. It presents the wishes and constraints on measurements for the purpose of validating the CAMS Radiation service. It lists the contacts made with possible providers of measurements and the data that have been obtained. Finally, it provides the list of stations whose data is being collected for the CAMS validation quarterly reports.

Validation should be periodically performed. One of the objectives is to monitor changes in quality from period to period. As a consequence, it is desirable to use the same group of measuring stations for validation, at least for several years to allow comparisons of performances and monitoring possible changes. The selected stations are located in several different climates as reported in the updated world map of the Köppen-Geiger climate classification by Peel et al. (2007). Figure 7.1 (Europe) and Figure 7.2 (other regions) show the location of the stations with their name and elevation above mean sea level used in 2017. Symbols code the initial summarization of the measurements: circle for 1 min, and downward triangle for 1 h. Colours code the type of data at each site: red for (*G, B, D*), yellow for (*G, B*), magenta for (*G, D*) and cyan for *G*, where *G, B*, *D*, stand respectively for global irradiance received on a horizontal surface, direct irradiance received on a surface normal to the direction of the sun, and diffuse irradiance received on a horizontal surface.

Depending on the provision of fresh data, possible problems affecting measuring instruments, possible rejection of some data by the quality control, and other causes, it is not always possible to use the same set of stations to perform the quarterly validation. Hence, the stations used the validation are mentioned in each validation report.

The validation is currently performed at a time step of 1 h for the global, diffuse and direct irradiances. The validation procedure is described in detail in each quarterly validation report. Each report documents how to cope with different time systems (universal time, true, solar time) and how to take care of the missing data. The procedure comprises two parts. In the first one, differences between estimates and observations are computed and then summarized by classical statistical quantities whose calculations are detailed. In the second part, statistical properties of estimates and observations are compared.

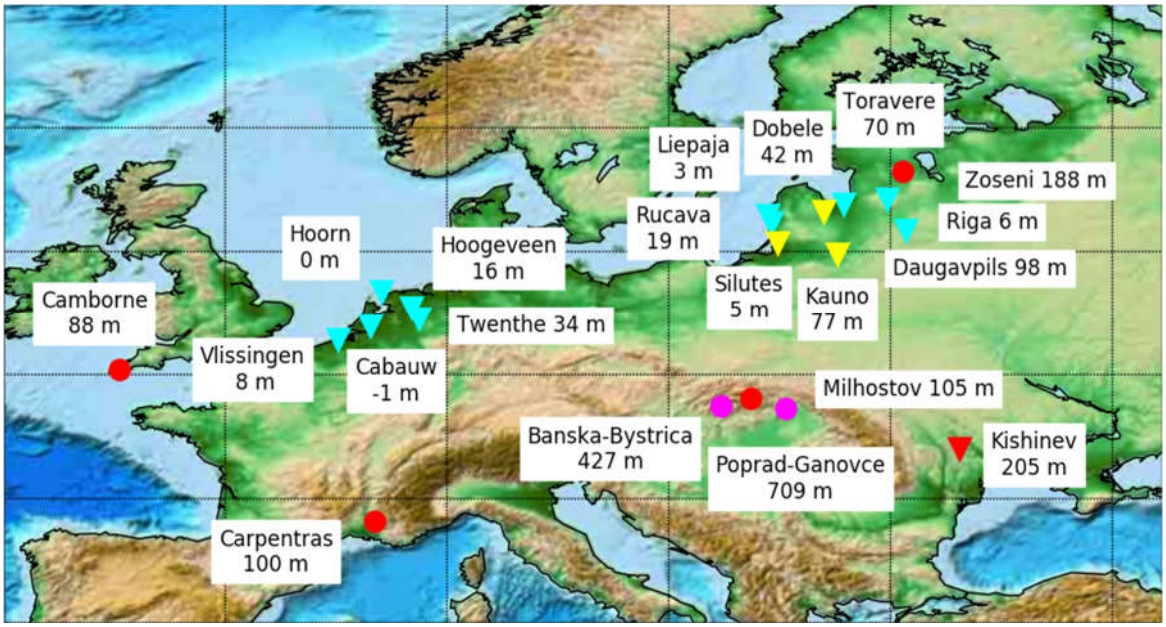

Figure 7.1. Map showing the stations in Europe. Symbols code the initial summarization: circle for 1 min, and downward triangle for 1 h. Colors code the type of data at each site: red for (*G, B, D*), yellow for (*G, B*), magenta for (*G, D*) and cyan for *G*.

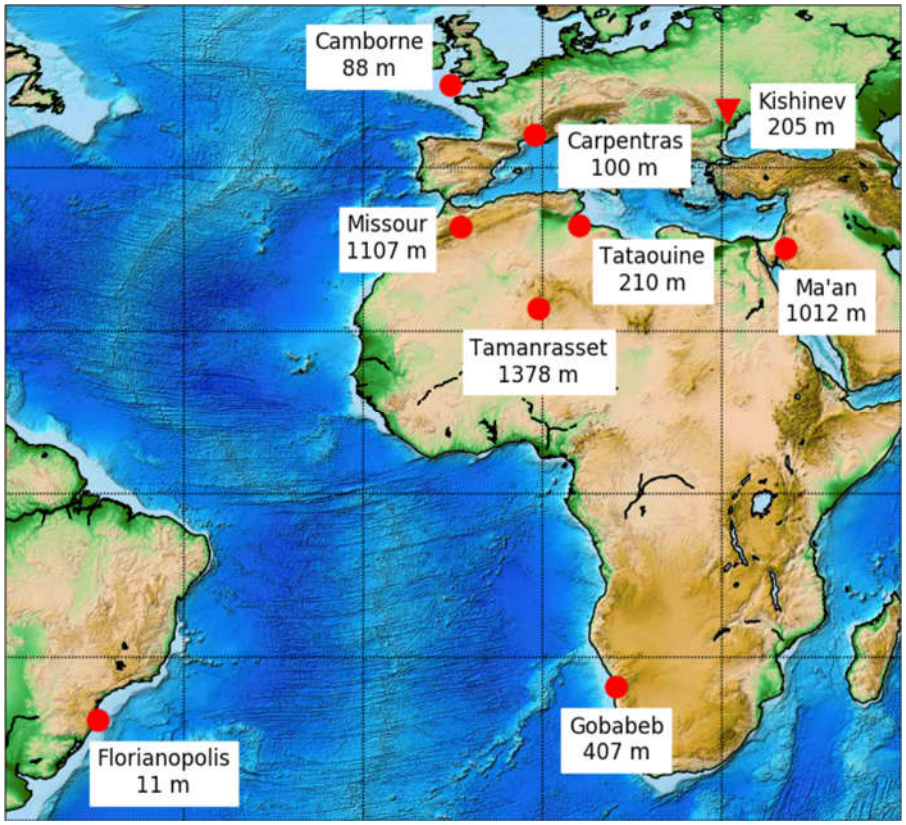

Figure 7.2. Map showing part of the stations. Symbols code the initial summarization: circle for 1 min, and downward triangle for 1 h. Colors code the type of data at each site: red for (*G, B, D*), yellow for (*G, B*), magenta for (*G, D*) and cyan for *G*.

The procedure for validation applies to irradiation or irradiance, and clearness index. The changes in solar radiation at the top of the atmosphere due to changes in geometry, namely the daily course of the sun and seasonal effects, are usually well reproduced by models and lead to a de facto correlation between observations and estimates of irradiation hiding potential weaknesses. The clearness index is a stricter indicator of the performances of a model regarding its ability to estimate the optical state of the atmosphere. Though the clearness index is not completely independent of the position of the sun, the dependency is much less pronounced than for radiation.

Quarterly validation reports can be found at
https://atmosphere.copernicus.eu/supplementary-services.
The results discussed in each report may be retrieved for several of the selected stations and others by running the service “Irradiation Validation Report” at the SoDa Web site:
http://www.soda-pro.com/fr/web-services/validation/irradiation-validation-report.

This service “Irradiation Validation Report” performs a comparison of the hourly or daily solar irradiation at surface estimated by the CAMS Radiation Service against several qualified ground measurements obtained from various sources. It returns a HTML page that contains statistics of comparison and graphs. Similar calculations can be done for the estimates from HelioClim-3 version 4 and HelioClim-3 version 5. The time coverage of the CAMS Radiation Service and HelioClim-3 version 5 databases is from 2004-02-01 up to 2 days behind real time, and up to d-1 for the HelioClim-3 version 4. Each station has its own temporal coverage of measurements, and the period of comparison must be selected within this period of data availability. The geographical coverage is the field of view of the Meteosat satellite, roughly speaking Europe, Africa, Atlantic Ocean, and Middle East (-66° to 66° in both latitudes and longitudes).

In addition, the validation of CAMS Radiation Service has been the subject of several scientific articles in Open Access:

- Marchand, M., Al-Azri, N., Ombe-Ndeffotsing, A., Wey, E., Wald, L.: Evaluating meso-scale change in performance of several databases of hourly surface irradiation in South-eastern Arabic Peninsula. Advances in Science and Research, 14, 7-15, doi:10.5194/asr-14-7-2017, 2017.
- Qu, Z., Oumbe, A., Blanc, P., Espinar, B., Gesell, G., Gschwind, B., Klüser, L., Lefèvre, M., Saboret, L., Schroedter-Homscheidt, M., Wald L.: Fast radiative transfer parameterisation for assessing the surface solar irradiance: The Heliosat-4 method, Meteorologische Zeitschrift, 26, 33-57, doi: 10.1127/metz/2016/0781, 2017.
- Thomas C., Wey E., Blanc P., Wald L., Validation of three satellite-derived databases of surface solar radiation using measurements performed at 42 stations in Brazil. Advances in Science and Research, 13, 81-86, doi:10.5194/asr-13-81-2016, 2016.

- Thomas, C., Wey, E., Blanc, P., Wald, L., and Lefèvre, M.: Validation of HelioClim-3 version 4, HelioClim-3 version 5 and MACC-RAD using 14 BSRN stations. SHC 2015, Istanbul, Turkey, 2-4 December 2015. Energy Procedia, 91, 1059-1069, 2016.
- Trolliet, M., Walawender, J.P., Bourlès, B., Boilley, A., Trentmann, J., Blanc, P., Lefèvre, M., and Wald, L.: Estimating downwelling solar irradiance at the surface of the tropical Atlantic Ocean: A comparison of PIRATA measurements against several re-analyses and satellite-derived data sets, Ocean Science, submitted, 2017.
- Trolliet, M., Walawender, J. P., Bourlès, B., Boilley, A., Trentmann, J., Blanc, P., Lefèvre, M., and Wald, L.: Downwelling surface solar irradiance in the tropical Atlantic Ocean: a comparison of re-analyses and satellite-derived data sets to PIRATA measurements, Ocean Sci., 14, 1021-1056, https://doi.org/10.5194/os-14-1021-2018, 2018.

Several articles focus on the McClear model:
Open Access

- Lefèvre, M., Oumbe, A., Blanc, P., Espinar, B., Gschwind, B., Qu, Z., Wald, L., Schroedter-Homscheidt, M., Hoyer-Klick, C., Arola, A., Benedetti, A., Kaiser, J. W., Morcrette, J.-J.: McClear: a new model estimating downwelling solar radiation at ground level in clear-sky condition. Atmospheric Measurement Techniques, 6, 2403-2418, doi: 10.5194/amt-6-2403-2013, 2013.
- Lefèvre, M., Wald, L.: Validation of the McClear clear-sky model in desert conditions with three stations in Israel. Advances in Science and Research, 13, 21-26, doi: 10.5194/asr-13-21-2016, 2016.
- Gschwind, B., Wald L., Blanc, P., Lefèvre, M., Schroedter-Homscheidt, M., Arola, A., 2019. Improving the McClear model estimating the downwelling solar radiation at ground level in cloud free conditions – McClear-V3., Meteorol. Z./Contrib. Atm. Sci., 28, 2, 147-163, doi:10.1127/metz/2019/0946.

Not Open Access

- Eissa, Y., Munawwar, S., Oumbe, A., Blanc, P., Ghedira, H., Wald, L., Bru, H., Goffe, D.: Validating surface downwelling solar irradiances estimated by the McClear model under cloud-free skies in the United Arab Emirates. Solar Energy, 114, 17-31, doi: 10.1016/j.solener.2015.01.017, 2015.

8. References

Anderson, G. P., S. A. Clough, F. X. Kneizys, J. H. Chetwynd, E. P. Shettle, 1986: AFGLatmospheric constituent profiles (0-120 km), Technical Report AFGL-TR-86-0110, AFGL(OPI), Hanscom AFB, MA. 01736.

Benedetti, A., J.-J. Morcrette, O. Boucher, A. Dethof, R. J. Engelen, M. Fischer, H. Flentjes, N. Huneeus, L. Jones, J. W. Kaiser, S. Kinne, A. Mangold, M. Razinger, A. J. Simmons, M. Suttie, and the GEMS-AER team, 2009. Aerosol analysis and forecast in the ECMWF Integrated Forecast System. Part II : Data assimilation. J. Geophys. Res., 114, D13205, doi:10.1029/2008JD011115.

Benedetti, A., J. W. Kaiser, J.-J. Morcrette, 2011: Global Climate. Aerosols [in" State of the Climate in 2010"], B. Am. Meteorol. Soc., 92(6), S65-S67.

Beyer H.-G., Costanzo C., and Heinemann D., 1996. Modifications of the Heliosat procedure for irradiance estimates from satellite images. Solar Energy, 56, 207-212.

Beyer H. G., Martinez J. P., Suri M., Torres J. L., Lorenz E., Hoyer-Klick C., Ineichen P., 2008. D 1.1.1 Handbook on Benchmarking, Management and Exploitation of Solar Resource Knowledge, CA – Contract No. 038665.

Bird, R., Hulstrom, R., 1981. Review, evaluatoin and improvement of direct irradiance models. Journal of Solar Energy Engineering 103, 182–192.

Blanc P., Wald L., 2012. The SG2 algorithm for a fast and accurate computation of the position of the Sun. Solar Energy, 86, 3072-3083, doi: 10.1016/j.solener.2012.07.018.

Blanc, P., B. Gschwind, M. Lefèvre, L. Wald, 2014: Twelve monthly maps of ground albedo parameters derived from MODIS data sets. In Proceedings of IGARSS 2014, held 13-18 July 2014, Quebec, Canada, USBKey, pp. 3270-3272.

Cano, D., Monget, J., Albuisson, M., Guillard, H., Regas, N., and Wald, L., 1986. A method for the determination of the global solar radiation from meteorological satellite data. Solar Energy, 37, 31-39.

Collins, W.D., P.J. Rasch, B.E. Eaton, B.V.Khattatov, J.-F. Lamarque, 2001. Simulating aerosols using a chemical transport model with assimilation of satellite aerosol retrievals: Methodology for INDOEX, J. Geophys. Res 106, D7, 7313-7336.

Diabaté L., Demarcq H., Michaud-Regas N., Wald L., 1988. Estimating incident solar radiation at the surface from images of the Earth transmitted by geostationary satellites: the Heliosat Project. International Journal of Solar Energy, 5, 261-278.

Diabaté L., Moussu G., Wald L., 1989. Description of an operational tool for determining global solar radiation at ground using geostationary satellite images. Solar Energy, 42(3), 201-207.

Eissa, Y., Munawwar, S., Oumbe, A., Blanc, P., Ghedira, H., Wald, L., Bru, H., and Goffe, D.: Validating surface downwelling solar irradiances estimated by the McClear model under

cloud-free skies in the United Arab Emirates, Solar Energy, 114, 17-31, 2015, doi:10.1016/j.solener.2015.01.017.

Espinar B., Ramírez L., Polo J., Zarzalejo L.F., Wald L., 2009. Analysis of the influences of uncertainties in input variables on the outcomes of the Heliosat-2 method. Solar Energy, 83, 1731-1741, doi:10.1016/j.solener.2009.06.010.

Farr T. G. et al. . The Shuttle Radar Topography Mission. Reviews of Geophysics. 45, RG, doi: 10.1029/2005RG000183(2007) (2004).

Geiger, M., Diabate, L., Menard, L., Wald, L., 2002. A web service for controlling the quality of measurements of global solar irradiation. Solar Energy 73, 475–480.

GEOSS, 2005. The Global Earth Observation System of Systems (GEOSS) 10-Year Implementation Plan (As adopted 16 February 2005), http://www.earthobservations.org/documents/10-Year%20Implementation%20Plan.pdf

Gesch, D.B., and Larson, K.S., 1996. Techniques for development of global 1-kilometer digital elevation models. In: Pecora Thirteen, Human Interactions with the Environment - Perspectives from Space, Sioux Falls, South Dakota, August 20-22, 1996.

Greuell, W., R. Roebeling, 2009: Toward a standard procedure for validation of satellite-derived cloud liquid water path: A study with SEVIRI data, J. Appl. Meteorol. Climatol., 48, 1575–1590.

Grüter W., Guillard H., Möser W., Monget J.M., Palz W., Raschke E., Reinhardt R.E., Schwarzmann P., Wald L., 1986. Solar radiation data from satellite images. Solar Energy R&D in the European Communities, series F: Solar Radiation Data, vol. 4, D. Reidel Publishing Co., 100 p.

Gschwind B., Ménard L., Albuisson M., Wald L., 2006. Converting a successful research project into a sustainable service: the case of the SoDa Web service. Environmental Modelling and Software, 21, 1555-1561, doi:10.1016/j.envsoft.2006.05.002.

Gschwind B., Wald L., Mahl R., Irigoin F., Ménard L., 2007. Test of several approaches for the composition of web services in meteorology. In Proceedings of EnviroInfo 2007, Environmental Informatics and systems research, the 21st International Conference on “Informatics for Environmental Protection”, Warsaw, Poland, 2007, vol. 1 “Plenary and session papers”, p. 127-133, ISBN 978-3-8322-6397-3.

Gschwind, B., Wald L., Blanc, P., Lefèvre, M., Schroedter-Homscheidt, M., Arola, A., 2019. Improving the McClear model estimating the downwelling solar radiation at ground level in cloud free conditions – McClear-V3., Meteorol. Z./Contrib. Atm. Sci., 28, 2, 147-163, doi:10.1127/metz/2019/0946.

Hammer, A., Heinemann, D., Westerhellweg, A., 1998. Derivation of Daylight and Solar Irradiance Data from Satellite Observations', Proceeding of the 9th Conference on Satellite Meteorology and Oceanography, Paris, France, 25.05.-29.05.1998, pp747-750, available at https://uol.de/fileadmin/user_upload/physik/ag/ehf/enmet/publications/solar/conferenc

e/1998/Derivation_of_Daylight_and_Solar_Irradiance_Data_from_Satellite_Observations.pdf.

Hess, M., P. Koepke, I. Schult, 1998: Optical properties of aerosols and clouds: The software package OPAC. B. Am. Meteorol. Soc., 79, 831–844.

Hoyer-Klick C., Schillings C., Schroedter Homscheidt M., Beyer H.-G., Dumortier D., Wald L., Menard L., Gschwind B., Martinoli M., Gaboardi E., Ramirez L., Polo J., Huld T., Suri M., Cebecauer T., De Blas M., Lorenz E., Pfatischer R., Remund J., Ineichen P., Tsvetkov A., Hofierka J., 2008. Management and exploitation of solar resource knowledge. Proceedings, EUROSUN 2008, 1st International Congress on Heating, Cooling and Buildings, Lisbon, Portugal (2008).

Hoyer-Klick, C., Schillings, C., Stökler, S., 2016. Satellite based estimation of solar radiation applied at DLR, SolarMedAtlas documentation available at http://www.solar-med-atlas.org/solarmed-atlas/download/DLR%20Heliosat%20Method.pdf.

Ineichen, P., Perez, R., 2002. A new airmass independent formulation for the Linke turbidity coefficient, Solar Energy, 73, 3, 151–157.

Inness, A., Baier, F., Benedetti, A., Bouarar, I., Chabrillat, S., Clark, H., Clerbaux, C., Coheur, P., Engelen, R.J., Errera, Q., Flemming, J., George, M., Granier, c., Hadji-Lazaro, J., Huijnen, V., Hurtmanns, D., Jones, L., Kaiser, J.W., Kapsomenakis, J., Lefever, K., Leitao, J., Razinger, M., Richter, A., Schultz, M.G., Simmons, A.J., Suttie, M., Stein, O., Thepaut, J.-N., Thouret, V., Vrekoussis, M., Zerefos, C., and the MACC team, 2013. The MACC reanalysis: an 8 yr data set of atmospheric composition. Atmos. Chem. Phys., 13, 8, 4073-4109, doi: 10.5194/acp-13-4073-2013.

Iqbal, M., 1983. An Introduction to Solar Radiation. Academic Press, New York.

ISO, 1995. Guide to the Expression of Uncertainty in Measurement, first ed. International Organization for Standardization, Geneva, Switzerland.

Kasten F., 1996. The Linke turbidity factor based on improved values of the integral Rayleigh optical thickness. Solar Energy, 56 (3), 239-244.

Kato, S., Ackerman, T. P., Mather, J. H., and Clothiaux, E. , 1999: The k–distribution method and correlated–k approximation for a shortwave radiative transfer model, J. Quant. Spectrosc. Radiat. Transfer, 62, 109–121.

Kinne, S., Holben, B., Eck, T., Smirnov, A., Dubovik, O., Dlutsker, I., Tanre, D., Zibozdi, G., Lohmann, U., Gahn, S., Easter, R., Chin, M., Ginoux, P., Takemaura, T., Tegen, I., Koch, D., Kahn, R., Vermote, E., Stowe, L., Torres, O., Mishchenko, M., Geogdzhayev, I., Hiragushi, A., 2001. How well do aerosol retrievals from satellites and representation in global circulation models match ground based Aeronet statistics. In: Beniston, M., Verstraete, M. (Eds.), Remote Sensing and Climate Modeling: Synergies and Limitations (Advances in Global Change Research. 7). Kluwer Academic Publishers, Dordrecht, pp. 103–158.

Kinne, S., Lohmann, U., Gahn, S., Easter, R., Chin, M., Ginoux, P., Takemura, T., Tegen, I., Koch, D., Herzog, M., Penner, J., Pitari, G., Holben, B., Eck, T., Smirnow, A., Dubovik, O., Slutsker,

I., Tanre, D., Torres, O., Mshchenk, M., Geoghzhayev, I., 2003. Monthly averages of aerosol properties: A global comparison among models, satellite data and aeronet ground data. Journal of Geophysical Research 108, D20.

Kinne, S., Schulz, M., Textor, C., Guibert, S., Balkanski, Y., Bauer, S., Bernsten, T., Berglen, T., Boucher, O., Chin, M., Collins, W., Dentener, F., Diehl, T., Easter, R., Feichter, J., Fillmore, D., Ghan, S., Ginoux, P., Gong, S., Grini, A., Hendricks, J., Herzog, M., Horowitz, L., Isaksen, I., Iversen, T., Kikevag, A., Kloster, S., Koch, D., Kristjansson, J., Krol, M., Lauer, A., Lamaraque, J., Lesins, G., Liux, X., Lohmann, U., Montanaro, V., Myhre, G., Penner, J., Pitari, G., Reddy, S., Seland, O., Stier, P., Takemura, T., Tie, X., 2006. An AeroCom initial assessment - optical properties in aerosol component modules of global models. Atmospheric Chemistry and Physics, 6, 1815-1834.

Klüser, L., Killius, N., Gesell, G., 2015: APOLLO_NG – a probabilistic interpretation of the APOLLO legacy for AVHRR heritage channels, Atmos. Meas. Tech., 8, 4155-4170.

Kriebel, K.T., R.W. Saunders and G. Gesell, 1989: Optical Properties of Clouds Derived from Fully Cloudy AVHRR Pixels. Beiträge zur Physik der Atmosphäre, Vol. 62, No. 3, pp. 165-171, August 1989

Kriebel K. T., Gesell G., Kästner M., Mannstein H., 2003: The cloud analysis tool APOLLO: Improvements and Validation, Int. J. Rem. Sens., 24, 2389-2408.

Laguarda, A., Giacosa, G., Alonso-Suarez, R., Abal, G., 2020: Performance of the site-adapted CAMS database and locally adjusted cloud index models for estimating global solar horizontal irradiation over the Pampa Húmeda, Sol. Energy, 199, 295-307, doi:/10.1016/j.solener.2020.02.005.

Lefèvre, M., and Wald, L., 2016: Validation of the McClear clear-sky model in desert conditions with three stations in Israel. Advances in Science and Research, 13, 21-26, doi:10.5194/asr-13-21-2016.

Lefèvre M., Diabaté L., Wald L., 2007. Using reduced data sets ISCCP-B2 from the Meteosat satellites to assess surface solar irradiance. Solar Energy, 81, 240-253, ddoi:10.1016/j.solener.2006.03.008.

Lefèvre, M., A. Oumbe, P. Blanc, B. Espinar, B. Gschwind, Z. Qu, L. Wald, M. Schroedter-Homscheidt, C. Hoyer-Klick, A. Arola, A. Benedetti, J. W. Kaiser, J.-J. Morcrette, 2013. McClear: a new model estimating downwelling solar radiation at ground level in clear-sky conditions. Atmospheric Measurement Techniques, 6, 2403-2418, doi: 10.5194/amt-6-2403-2013.

Liu, H., Pinker, R.T., 2005. A global view of aerosols from merged transport models, satellite and ground observations. Journal of Geophysical Research 110, D10S15.

Marchand, M., Al-Azri, N., Ombe-Ndeffotsing, A., Wey, E., and Wald, L., 2017: Evaluating meso-scale change in performance of several databases of hourly surface irradiation in South-eastern Arabic Peninsula, Adv Sci Res, 14, 7-15, doi:10.5194/asr-14-7-2017.

Mayer, B., A. Kylling, 2005: Technical note: The libRadtran software package for radiative transfer calculations - description and examples of use, Atmos. Chem. Phys., 5, 1855-1877, doi:10.5194/acp-5-1855-2005.

McPeters, R., Bhartia, P., Krueger, A., Herman, C., Wellmeyer, C., Seftor, C., Jaross, G., Torres, O., Moy, L., Labow, G., Byerly,W.,Taylor, S., Swissler,T., Cebula, R., 1998. Earth probe total ozone mapping spectrometer (toms) dataproducts user's guide.Tech.rep., NASATechnical Publication 1998-206895.

Ménard L., Wald L., Blanc Ph., Ranchin T., 2009. Sitting of a solar power plant: development of Web service based on GEOSS data and guidance. In: Proceedings, 33rd International Symposium on Remote Sensing of Environment, ISRSE 33, Stresa, Italy, May 4-8, 2009, paper 789, [USB key].

Morcrette, J.-J., O. Boucher, L. Jones, D. Salmond, P. Bechtold, A. Beljaars, A. Benedetti, A. Bonet, J. W. Kaiser, M. Razinger, M. Schulz, S. Serrar, A. J. Simmons, M. Sofiev, M. Suttie, A. M. Tompkins, and A. Untch (2009): Aerosol analysis and forecast in the ECMWF Integrated Forecast System. Part I: Forward modelling, J. Geophys. Res., 114D, D06206, doi:10.1029/2008JD011235.

Möser, W. and Raschke, E., 1984. Incident solar radiation over Europe estimated from Meteosat data. Journal of Applied Meteorology, 23, 166-170.

Mueller, R., Dagestad, K., Ineichen, P., Schroedter, M., Cros, S., Dumortier, D., Kuhlemann, R., Olseth, J., Piernavieja, G., Reise, C., Wald, L., and Heinnemann, D., 2004. Rethinking satellite based solar irradiance modelling - the SOLIS clear sky module. Remote Sensing of Environment, 91, 160-174.

Ohmura, A., Gilgen, H., Hegner, H., Mueller, G., Wild, M., Dutton, E. G., Forgan, B., Froelich, C., Philipona, R., Heimo, A., Koenig-Langlo, G., McArthur, B., Pinker, R., Whitlock, C. H., and Dehne, K. , 1998: Baseline Surface Radiation Network (BSRN/WCRP): New precision radiometry for climate research, B. Am. Meteorol. Soc., 79, 2115–2136, doi:10.1175/15200477(1998)079<2115:BSRNBW>2.0.CO;2.

Oumbe A., 2009. Exploitation des nouvelles capacités d'observation de la terre pour évaluer le rayonnement solaire incident au sol (Assessment of solar surface radiation using new earth observation capabilities). Thèse de Doctorat, MINES ParisTech, Paris, France, 128 pages).

Oumbe, A., Qu, Z., Blanc, P., Bru, H., Lefèvre, M., and Wald, L., 2012: Modeling circumsolar irradiance to adjust beam irradiances from radiative transfer models to measurements, EMS Annual Meeting 2012, 10–14 September 2012, Lodz, Poland.

Oumbe, A., Qu, Z., Blanc, P., Lefèvre, M., Wald, L., and Cros, S., 2014: Decoupling the effects of clear atmosphere and clouds to simplify calculations of the broadband solar irradiance at ground level. Geoscientific Model Development, 7, 1661-1669, doi:10.5194/gmd-7-1661-2014. Corrigendum, 7, 2409-2409, 2014.

Peel, M. C., Finlayson, B. L., McMahon, T. A., 2007: Updated world map of the Köppen-Geiger climate classification. Hydrol. Earth Syst. Sci., 11, 1633-1644.

Perez R., Seals R., Zelenka A., 1997. Comparing satellite remote sensing and ground network measurements for the production of site/time specific irradiance data. Solar Energy, 60, 89–96.

Qu, Z., Gschwind, B., Lefevre, M., and Wald, L., 2014: Improving HelioClim-3 estimates of surface solar irradiance using the McClear clear-sky model and recent advances in atmosphere composition. Atmospheric Measurements Techniques, 7, 3927–3933, doi:10.5194/amt-7-3927-2014.

Qu, Z., Oumbe, A., Blanc, P., Espinar, B., Gesell, G., Gschwind, B., Klüser, L., Lefèvre, M., Saboret, L., Schroedter-Homscheidt, M., and Wald L.., 2017. Fast radiative transfer parameterisation for assessing the surface solar irradiance: The Heliosat-4 method, Meteorologische Zeitschrift, 26, 33-57, doi: 10.1127/metz/2016/0781.

Reinhardt, B., R. Buras, L. Bugliaro, B. Mayer, S. Wilbert, 2012: Circumsolar radiation- a reason for solar resource overestimation – Globally characterized, EMS Annual Meeting 2012, 10-14 September 2012, Lodz, Poland.

Remund J., Wald L., Lefèvre M., Ranchin T., Page J., 2003. Worldwide Linke turbidity information. In Proceedings of ISES Solar World Congress, 16-19 June, Göteborg, Sweden, CD-ROM published by International Solar Energy Society.

Remy, S., Z. Kipling, J. Flemming, O. Boucher, P. Nabat, M. Michou, A. Bozzo, M. Ades, V. Huijnen, A. Benedetti, R. Engelen, V.-H. Peuch, J.-J. Morcrette, 2019: Description and evaluation of the tropospheric aerosol scheme in the Integrated Forecasting System (IFS-AER, cycle 45R1) of ECMWF, Geosci. Model. Dev., 12, 4627-4659, doi:10.5194/gmd-12-4627-2019.

Rigollier C., Bauer O., Wald L., 2000. On the clear sky model of the 4th European Solar Radiation Atlas with respect to the Heliosat method. Solar Energy, 68(1), 33-48.

Rigollier C., Lefèvre M., Wald L., 2004. The method Heliosat-2 for deriving shortwave solar radiation from satellite images. Solar Energy, 77(2), 159-169.

Schade, N. H., A. Macke, H. Sandmann, C. Stick, 2007: Enhanced solar global irradiance during cloudy sky conditions. Meteor. Z., 16, 295–304.

Schaaf, C. B., F. Gao, A. H. Strahler, W. Lucht, X. W. Li, T. Tsang, N. C. Strugnell, X. Y. Zhang, Y. F. Jin, J. P. Muller, P. Lewis, M. Barnsley, P. Hobson, M. Disney, G. Roberts, M. Dunderdale, C. Doll, R. P. d'Entremont, B. X. Hu, S. L. Liang, J. L. Privette, D. Roy, 2002: First operational BRDF, albedo nadir reflectance products from MODIS, Remote Sens. Environ., 83, 135-148, doi:10.1016/S0034-4257(02)00091-3.

Schutgens, N. A. J., R. A. Roebeling, 2009: Validating the validation: the influence of liquid water distribution in clouds on the intercomparison of satellite and surface observations, J. Atmos. Oceanic Technol., 26, 1457–74, doi: 10.1175/2009jtecha1226.1.

Shiobara, M., S. Asano, 1993: Estimation of cirrus optical thickness from sun photometer measurements, J. Appl. Meteor., 33, 672-681, doi: 10.1175/1520-0450(1994)033<0672:EOCOTF>2.0.CO;2.

Tarpley, J., 1979. Estimating incident solar radiation at the surface from geostationary satellite data. Journal of Applied Meteorology, 18, 1172-1181.

Tegen, I., Hollring, P., Chin, I., Fung, D., D., J., Penner, J., 1997. Contribution of different aerosol species to the global aerosol extinction optical thickness: Estimates from model results. Journal of Geophysical Research 102, 23895–23915.

Thomas, C., Wey, E., Blanc, P., Wald, L., and Lefèvre, M., 2016a: Validation of HelioClim-3 version 4, HelioClim-3 version 5 and MACC-RAD using 14 BSRN stations, Energy Procedia, 91, 1059-1069, doi: 10.1016/j.egypro.2016.06.275.

Thomas, C., Wey, E., Blanc, P., and Wald, L., 2016b: Validation of three satellite-derived databases of surface solar radiation using measurements performed at 42 stations in Brazil, Adv Sci Res, 13, 81-86, doi:10.5194/asr-13-81-2016.

Vermote, E.F., D. Tanré, J. L. Deuzé, M. Herman, J.-J. Morcrette, 1997: Second simulation of the satellite signal in the solar spectrum: An overview, IEEE T. Geosci. Remote Sens., 35, 675–686.

Wahab, A. M., El Metwally M., Hassan R., Lefèvre M., Oumbe A., Wald L., 2009. Assessing surface solar irradiance in Northern Africa desert climate and its long-term variations from Meteosat images. International Journal of Remote Sensing, 31(01), 261-280.

Wald L., Albuisson M., Best C., Delamare C., Dumortier D., Gaboardi E., Hammer A., Heinemann D., Kift R., Kunz S., Lefèvre M., Leroy S., Martinoli M., Ménard L., Page J., Prager T., Ratto C., Reise C., Remund J., Rimoczi-Paal A., Van der Goot E., Vanroy F., and Webb A., 2002. SoDa: a project for the integration and exploitation of networked solar radiation databases. In: Environmental Communication in the Information Society, W. Pillmann, K. Tochtermann Eds, Part 2, pp. 713-720. Published by the International Society for Environmental Protection, Vienna, Austria.

Wald L., Albuisson M., Best C., Delamare C., Dumortier D., Gaboardi E., Hammer A., Heinemann D., Kift R., Kunz S., Lefèvre M., Leroy S., Martinoli M., Ménard L., Page J., Prager T., Ratto C., Reise C., Remund J., Rimoczi-Paal A., Van der Goot E., Vanroy F., and Webb A., 2004. SoDa: a Web service on solar radiation. In Proceedings of Eurosun 2004, published by PSE GmbH, Freiburg, Germany, pp. (3)921-927, ISBN 3-9809656-4-3.

WMO, 1981. Technical Note N° 172, WMO-No. 554, World Meteorological Organization, Geneva, Switzerland, pp. 121-123.

WMO: Guide to meteorological instruments and methods of observation, WMO-No 8, 2008 edition updated in 2010, World Meteorological Organization, Geneva, Switzerland, 2012.

Zelenka A., Perez R., Seals R., Renne´ D., 1999. Effective accuracy of satellite-derived hourly irradiances. Theoretical and Applied Climatology, 62, 199–207.

Zender, C. S., H. Bian, and D. Newman, 2003. Mineral Dust Entrainment And Deposition (DEAD) model: Description and 1990s dust climatology. J. Geophys. Res., 108(D14), 4416, doi:10.1029/2002JD002775.

Copernicus Atmosphere Monitoring Service

ECMWF - Shinfield Park, Reading RG2 9AX, UK

Contact: info@copernicus-atmosphere.eu